AD-A153 320 SIMULATION OF AIRCRAFT BEHAVIOUR ON AND CLOSE TO THE GROUND(U) ADVISORY GROUP FOR AEROSPACE RESEARCH AND DEVELOPMENT NEUILLY-SUR-SEINE (FRANCE) 1/1

UNCLASSIFIED A G BARNES ET AL. JAN 85 AGARD-AG-285 F/G 1/2 NL

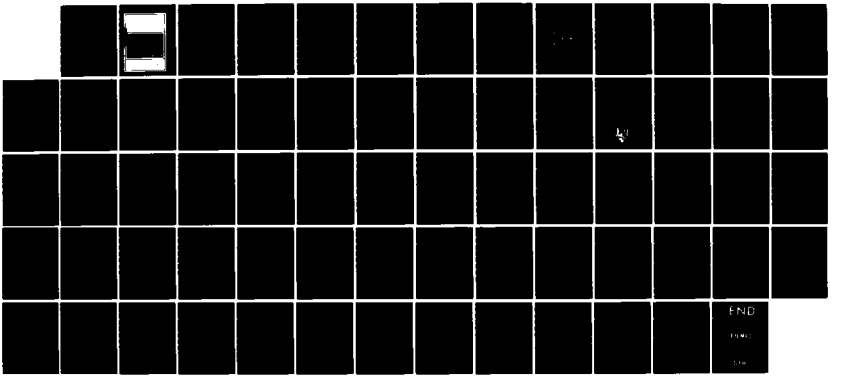

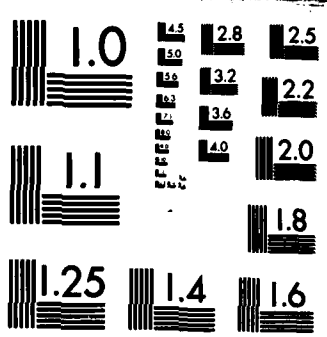

AGARD-AG-285

AGARD

ADVISORY GROUP FOR AEROSPACE RESEARCH & DEVELOPMENT

AGARDograph No.285

Simulation of Aircraft Behaviour on and Close to the Ground

NORTH ATLANTIC TREATY ORGANIZATION

AGARD-AG-285

NORTH ATLANTIC TREATY ORGANIZATION

ADVISORY GROUP FOR AEROSPACE RESEARCH AND DEVELOPMENT

(ORGANISATION DU TRAITE DE L'ATLANTIQUE NORD)

AGARDograph No.285

SIMULATION OF AIRCRAFT BEHAVIOUR ON AND CLOSE TO THE GROUND

by

A.G.Barnes
British Aerospace Plc
Warton Division
Preston, Lancs PR4 1AX
UK

and

T.J.Yager
Aerospace Technologist
Impact Dynamics Office — MS 497
NASA — Langley Research Center
Hampton VA 23665
USA

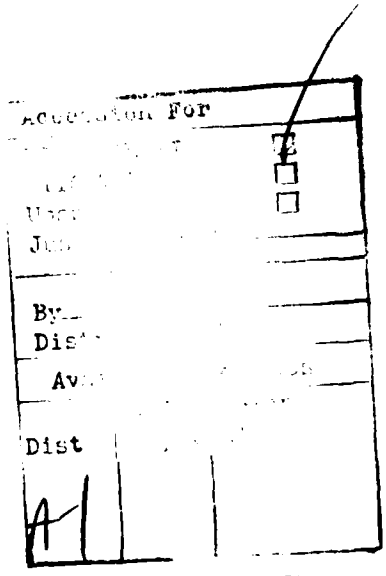

This AGARDograph has been sponsored by the Flight Mechanics Panel of AGARD.

THE MISSION OF AGARD

The mission of AGARD is to bring together the leading personalities of the NATO nations in the fields of science and technology relating to aerospace for the following purposes:

- Exchanging of scientific and technical information;
- Continuously stimulating advances in the aerospace sciences relevant to strengthening the common defence posture;
- Improving the co-operation among member nations in aerospace research and development;
- Providing scientific and technical advice and assistance to the North Atlantic Military Committee in the field of aerospace research and development;
- Rendering scientific and technical assistance, as requested, to other NATO bodies and to member nations in connection with research and development problems in the aerospace field;
- Providing assistance to member nations for the purpose of increasing their scientific and technical potential;
- Recommending effective ways for the member nations to use their research and development capabilities for the common benefit of the NATO community.

The highest authority within AGARD is the National Delegates Board consisting of officially appointed senior representatives from each member nation. The mission of AGARD is carried out through the Panels which are composed of experts appointed by the National Delegates, the Consultant and Exchange Programme and the Aerospace Applications Studies Programme. The results of AGARD work are reported to the member nations and the NATO Authorities through the AGARD series of publications of which this is one.

Participation in AGARD activities is by invitation only and is normally limited to citizens of the NATO nations.

Published January 1985

ISBN 92-835-1490-4

Printed by Specialised Printing Services Limited
40 Chigwell Lane, Loughton, Essex IG10 3TZ

PREFACE

Widespread use is already made of ground-based simulation in aeronautical research, aircraft design and development, and for pilot training. As standards of representation of aircraft systems, their behaviour and their environment improve, the potential benefits of ground-based simulator operations, as a substitute for flight, will continue to increase. Recently, major efforts have been made to expand the simulation envelope of fixed-wing aircraft to include modelling of aircraft operations on and close to the ground. The advent of modern digital computer processing has enabled the mathematical representation of complex tyre/runway dynamics and friction characteristics to be adequately addressed in real time.

This AGARDograph provides a guide to the current state of the technology of simulating fixed-wing aircraft handling qualities and performance on or close to the ground, and indicates some of the pitfalls which may prevent an adequate implementation. The scope of possible applications in both aircraft design work and pilot training is indicated and the requirements for mathematical model definitions and implementations are discussed. The current requirements for visual and motion systems, cockpit cueing, and software modelling are also reviewed, and illustrated with specific examples in areas of aircraft research and development studies and pilot training uses. The report conclusions identify needs for further improvements and additional data acquisition.

CONTENTS

SIMULATION OF AIRCRAFT BEHAVIOUR

ON AND CLOSE TO THE GROUND

1.0 Introduction

Widespread use is made of ground-based flight simulation in aeronautical research, aircraft design and development, and for pilot training. As the standards achieved in representing the behaviour of the aircraft systems and their operating environment are being continually improved, the potential benefits from ground based simulator operations, as a substitute for flight, are being increased and expanded. Reference 1 quantifies some of these benefits, based on data published in the period 1980-81. Not the least of these benefits are the reductions in operating costs which the use of ground-based simulators brings. The median ratio of simulator operating costs to aircraft operating costs quoted in reference 1 is 0.08, compared to 0.12 based on 1976-78 data. Typically, an F-4D aircraft simulator, achieves a ratio of 0.075, comprising $2,400 per hour to fly the aircraft and $180 per hour to fly the simulator. Military flying costs are in the range of $1000 - $6000 per hour. It hardly needs to be said that the more expensive and complicated the aircraft, the smaller the ratio of simulator to aircraft operating costs.

Aircraft crew flight training costs are rising dramatically each year. Reference 2 indicates that for a small jet trainer, "extra hour" training costs are $1650 per hour and full training costs are $4000 per hour. At the same time, the cost of a simulator, on a task for task basis, is not changing.

Reference 1 also draws attention to the concept of the Training Effectiveness Ratio, TER, which is a qualitative measure of the carry-over to flight of skills acquired in the simulator. If the simulator has no training value for a particular task, this ratio is zero; in some circumstances, where more intensive training can be achieved in the simulator than in flight, the ratio can be much greater than unity. Reference 1 shows that the TER varies widely with the intended use of the simulator, and a typical median value is 0.5.

Over the past few years, there has been a gradual increase in TER values, partly because of the improvements in the standard to which a particular phase of flight can be represented, and partly because the simulator can encompass flight segments which previously could not be managed.

Simulating the operation of aircraft on and in close proximity to the ground imposes considerable demands on equipment, even today. Such operations are of vital interest to research, design, and operation of both civil and military aircraft. To be able to represent them with confidence will further add to the TER values, both by giving improved realism to tasks already available in simulators, and by expanding the range of investigations and training situations which are amenable to ground-based trials. This report is intended (a) to provide a guide to the current state of simulation technology for representing aircraft handling and performance on or close to the ground, and (b) to indicate some of the pitfalls which are present in an adequate implemention of this technology. The scope of the report is limited to fixed wing aircraft.

2.0 Applications

Before discussing the present capability of ground based simulators in representing the behaviour of an aircraft on the ground, it is useful to itemise the research and training activities which would benefit from a good standard of simulation. Tasks which would normally apply only to civil aircraft operations are identified by - (C); tasks which would normally apply only to military aircraft operations are identified by - (M). Others apply to both military and civil operations.

2.1 Aircraft Research and Development

2.1.1 Longitudinal Stability and Control

* Nose-wheel lift in take-off run.
* Pitch control to achieve correct attitude for take-off.
* Transition at unstick.
* Take-off handling through c.g. range.
* Pitch control in landing flare.
* Undercarriage dynamics/structural coupling during ground roll.

2.1.2 Longitudinal Performance

* Accelerate/stop performance.
* Take-off distance-variation with configuration
* Take-off distance-variation with runway surface, wind and climatic conditions. (C)
* Catapult from aircraft carriers (M).
* Ski-jump capability (M).
* Steep approach/no flare techniques (M).
* Short landing techniques (M).
* Landing distance variation with runway surface, wind and climatic conditions (C).
* Benefit of deceleration devices (Wheelbrakes, thrust reversers, parachute).
* Undercarriage and tyre design.

2.1.3 Lateral Stability and Control

* Taxiing manoeuvres, nose-wheel steering design.
* Lateral stability in ground roll.
* Influence of undercarriage geometry and tyre forces on steering.
* Transients at unstick in crosswinds.
* Cross wind landing technique.
* Influence of thrust reverser on stability.

2.1.4 Lateral Performance

* Touchdown dispersion.
* Directional control in ground run.
* Effect of runway surface and winds on directional control.
* Operational limits.
* Landing on narrow strips (dispersed operation) (M)

2.2 Pilot Training

2.2.1 Take-off

* Push back, taxi and holding procedures (C).
* Standard and high weight take-offs.
* Minimum field length, hot and high (C).
* Emergency procedures during take-off.
* Effects of wind and weather.
* Aborted take-off.
* Post take-off procedures, noise abatement (C).
* Scramble take-off. (M)

2.2.2 Landing/Ground Roll

* Flare techniques
* Precautionary landing (M)
* Max-weight, hot and high operation.
* Use of de-celeration devices.
* Engine-out cases.
* Landing with systems failed.
* Effects of wind and weather.
* Effects of runway surface and gradient.
* Taxi-ing, parking, shut-down.

3.0 Modelling Considerations

3.1 General

To simulate an aircraft in flight, a mathematical representation is required such as described in reference 3. In its simplest form six simultaneous linear differential equations are solved, to represent the six degrees of freedom of the aircraft. The coefficients of these equations include quasi-static aerodynamic derivatives, which determine the stability and control of the aircraft. Classical methods of analysis may be used to determine the modal properties of these equations, and allow the flying qualities of the aircraft to be related to the description of the aircraft implicit in the model.

A better representation of an aircraft in flight is given by restating the aircraft equations of motion to permit large perturbation manoeuvres. The equations are no longer linear, and the aerodynamic characteristics are no longer expressed in derivative form. The forces and moments due to aerodynamic effects are expressed as functions of many parameters - speed, incidence, Mach No., and so on. The influence of air density is also represented. These equations may be used to derive the position and orientation of the aircraft in space, together with its rotational and translational accelerations and rates. An extension to these equations allows the inclusion of movements of the air-mass with respect to the aircraft and the ground. Consequently, the

effects of turbulence and of steady winds on the pilot's ability to control the aircraft, and on his ability to perform a given task, can be examined.

At first sight, it would be assumed that the most comprehensive set of equations is the one to use, provided that mechanisation difficulties do not intrude, since the model will most closely represent the real situation. However, in research and development, the intended use of the simulation determines the choice of model. An over-complex model will not be suitable for parametric studies, since the response will be dependent on amplitude, and will be highly complex. Moreover, a complex formulation of the model is only worthwhile if the model input data is sufficiently accurate and detailed.

The methods used to model an aircraft in flight apply equally well to the modelling of a vehicle moving on the ground. The model itself will be more complex, since the assumption of small perturbations from a steady state would be unduly restrictive. More degrees of freedom are needed, allowing the tyres, wheels, suspension, and steering to be simulated. The special properties of the ground surface, as well as the aerodynamic effects as speed increases must also be reproduced. In particular, precipitation affects the performance of the aircraft on the ground (Figure 1).

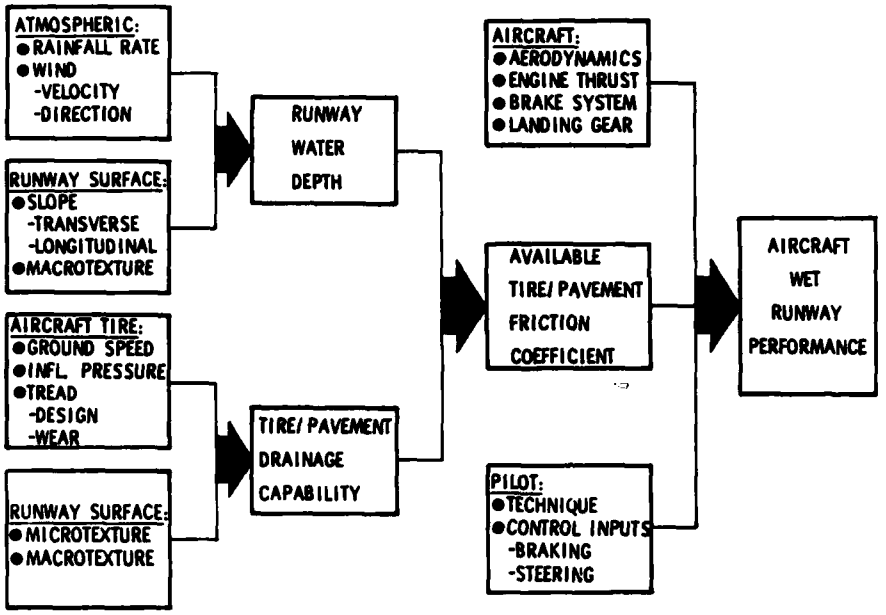

Figure 1 Factors affecting aircraft wet runway performance

The ability to simulate take-off and landing emerges when the fully airborne model and the representative ground-roll model are combined. In doing so, care must be taken to ensure that the aerodynamic changes associated with flight close to the ground are included, as non-linear incremental lift, drag and pitching moments. The complexity of the computation is influenced by the choice of axis system. A further consideration, and one which has delayed accurate representaton of take-off, landing and ground-roll, is the magnitude of the computing task, both in terms of computer speed and computer capacity. In the past analog computers had the former attribute, but not the latter, and digital computers had the latter but not the former. Hybrid configurations were used successfully until the computer technology of the past few years made digital processing the preferred method of solving the mathematical representation of the aircraft in real time.

The technical literature abounds with references to the modelling of vehicles in contact with the ground and the associated suspension systems. References 4 and 5 are good starting points for the identification of such models.

3.2 Model Implementation

The elements to be considered in modelling an aircraft in contact with the ground are seen in block diagram form on figure 2. The breakdown inside the computer shows the individual elements which must be represented; each element requires information from, or supplies information to the other elements. The elements themselves may be modelled to different levels of complexity, depending on the application of the simulation. To allow further examination of this block diagram, Appendix A contains a listing of the terms used in the equations of motion which the computer must solve. Appendix B contains the generalized equations necessary for modelling aircraft in ground roll.

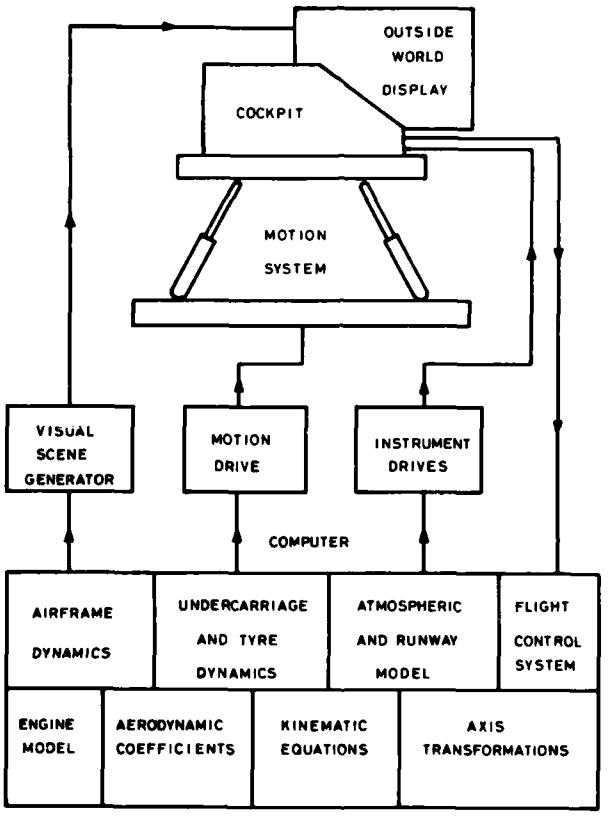

Figure 2 Aircraft modelling block diagram

The next step towards the successful simulation of the handling of an aircraft on the ground is to gather together the data sets which are required to solve the equations of motion. Of particular importance is the accuracy with which the tyre friction envelope, including free rolling, braking, cornering, and combinations thereof, can be defined under a variety of loading, speed and environmental conditions. Aircraft tyre friction performance is influenced by many factors including tyre runway surface characteristics, aircraft landing gear geometry, and brake system performance. NASA, Langley test results (references 6 - 9) have provided sufficient friction data on a large number of different - sized pneumatic tyres to permit determination of empirically derived equations and relationships for use in estimating a particular tyre friction performance. Figure 3 indicates how this methodology is used to transform tyre friction - speed gradient data obtained experimentally in one operational mode (e.g. from a ground vehicle locked wheel test) into an estimate of the variation of aircraft tyre locked wheel skidding (μ_{skid}), maximum friction (μ_{max}), and side friction (μ_{side}) coefficients, with speed. Using an anti-skid braking efficiency term (η), the estimated aircraft tyre effective braking friction coefficient (μ_{eff}) variation with speed can be determined from the derived maximum friction values. A typical match between theory and experiment is seen on figure 4.
The undercarriage representation is unique to the type of aircraft which is simulated. Travels are dictated by mechanical design; static and dynamic behaviour is determined by the choice of springing and also damping. Typical curves (from reference 4) of the main and nose gear stiffness characteristics of a fighter aircraft are seen on figures 5 and 6. Figure 7 shows the characteristics of the oleo and two stage damping valve.

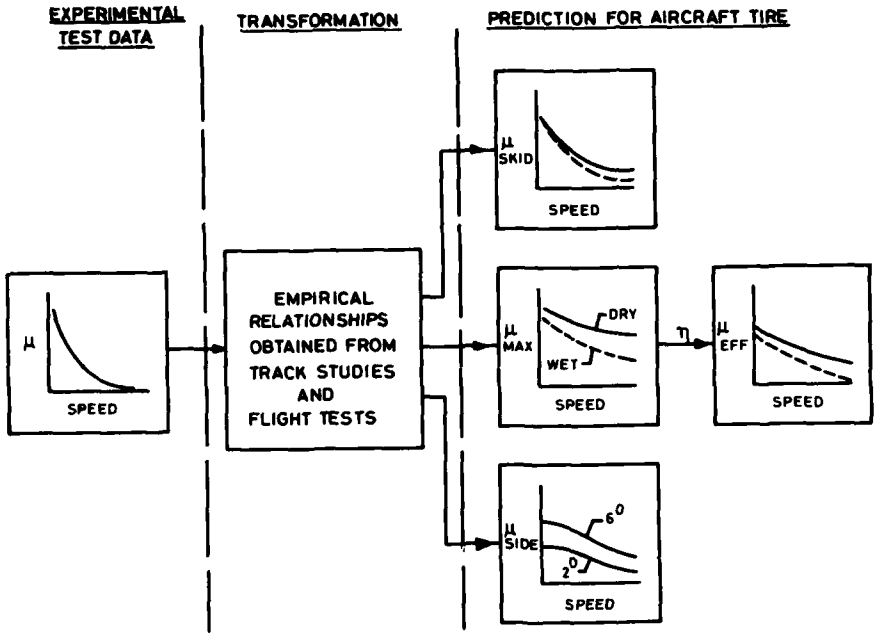

Figure 3 Methodology used to estimate aircraft tire friction performance

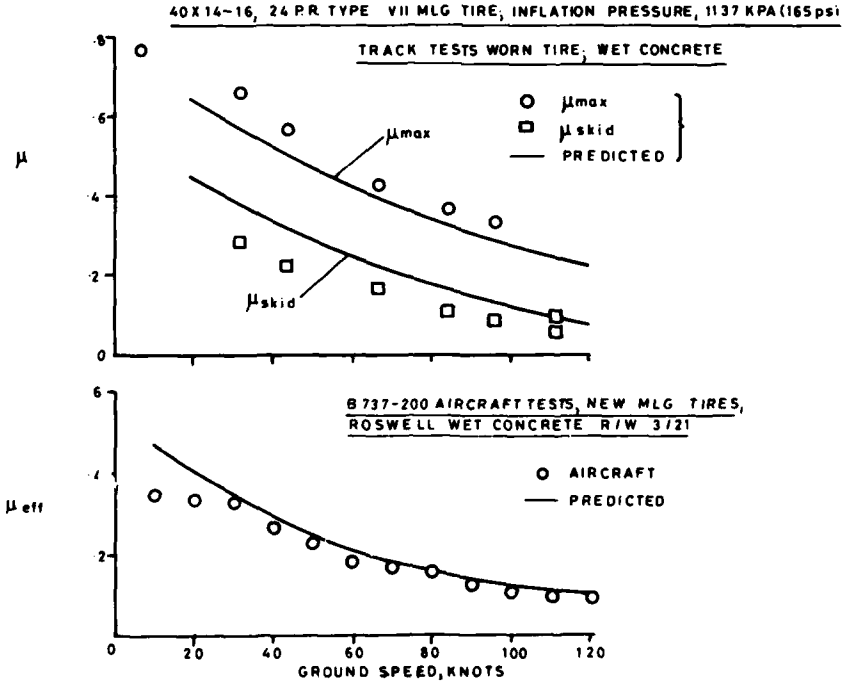

Figure 4 Agreement between experimental braking performance and theory prediction

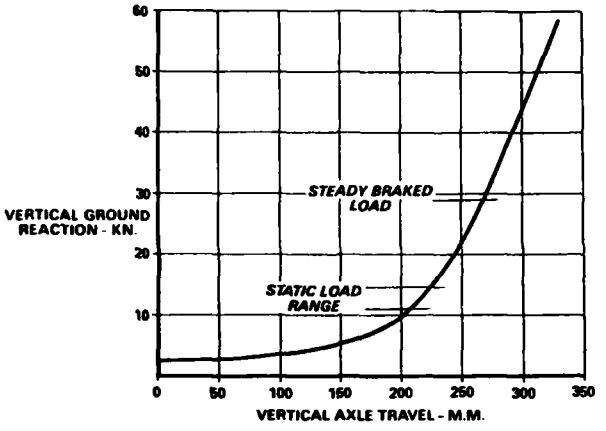

Figure 5 Nose undercarriage ground spring curve

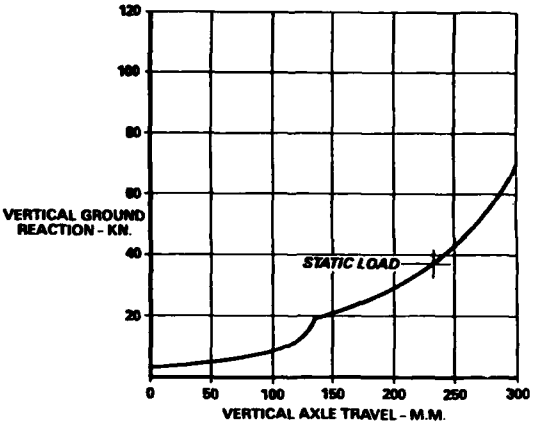

Figure 6 Main undercarriage ground spring curve

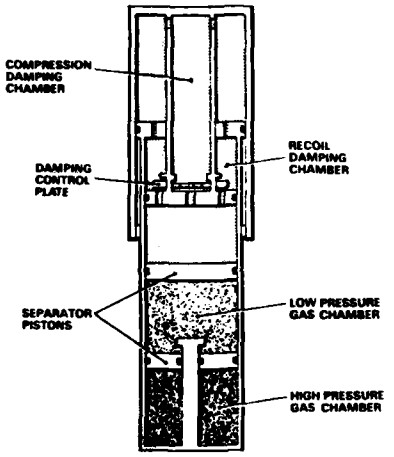

Figure 7a Diagrammatic arrangement of Jaguar main shock absorber

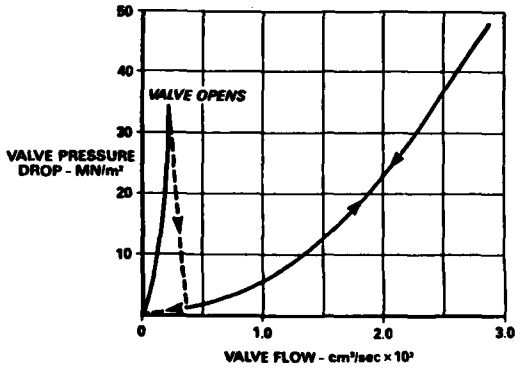

Figure 7b Pressure versus flow characteristic of a two-stage damping valve

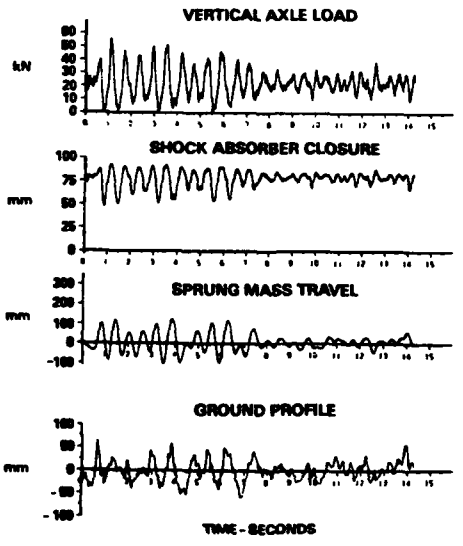

Figure 8 Main undercarriage response over rough ground Unit load = 2427 kg Speed = 120 kts

When these component descriptions are introduced into the computer model of the aircraft in contact with the ground, dynamic response calculations are possible. Figure 8 shows the loads and travel of the undercarriage, and the vertical movements of the aircraft, when running at constant speed over rought ground.

4.0 Simulator Technology

4.1 Visual Systems

4.1.1 General Remarks

Providing the pilot with a visual representation of the world from the cockpit during flight is the most demanding aspect of any advanced flight simulator. The conflicting requirements of wide field of view, good resolution, high brightness, good scene detail, and fast dynamic response cannot all be met by existing equipments. The most complete discussion of these requirements and their various trade-offs is contained in reference 10. The need to represent flight in close proximity to the ground exaggerates the problems which the visual display designer faces. Fortunately, these problems are eased in the ground-borne case by the restrictions in aircraft motions due to ground restraint, and by the relatively low speeds associated with take-off, landing, and ground roll.

Visual display options for take-off and landing are reviewed in reference 11. Table 1 from that reference compares the strength and weakness of 7 display systems. Since the report was written, progress in computer generated image (CGI) systems has established their superiority for applications where cost is not the over-riding factor. Even so, the deficiencies implied by the table still exist.

Table 1 Visual displays for approach and landing

GROUP \ FACTOR	FIELD OF VIEW	TEXTURAL QUALITY	RESOLUTION	RESPONSE TO INPUTS	RANGE	FLEXIBILITY	INSTALLATION OVERHEAD (6)	CAPITAL COST
RASTER TV/MODEL	E 1)	B 3)	D	D	D	D	HIGH	MODERATE +
FILM/SERVO PROJECTOR	E	B	A	D	D	E	MODERATE	MODERATE
LASER TV/MODEL (PREDICTED)	C 2)	B	A	D	B	D	HIGH	HIGH
NIGHT CGI	C 2)	D 4)	B	B	B	D	LOW	MODERATE -
NIGHT CGI WITH RASTER INFILL	C 2)	C	B	B	B	D	LOW	MODERATE
DAY CGI	C 2)	D	C	B 5)	C	B	MODERATE -	HIGH
CONTACT ANALOG	C 2)	E	C	A	E	D	LOW -	LOW

SCALE A B C D E
EXCELLENT — BARELY ACCEPTABLE

NOTES:
1. One window
2. Three window
3. Modelling limit
4. No credit for neon signs and firework displays
5. Subject to good cycle time
6. Space, power consumption

In the case of daylight CGI systems, the principal complaint is the cartoon-like quality of the images, and the lack of fine detail. The introduction of textured surfaces is a considerable improvement in this respect. Nor does a solution seem to be in sight to the problem of estimating distance accurately with simulator visual systems, particularly when the objects are in the range 10-100m. Although the visual system may be perfect from geometrical considerations such as perspective and object size, the current methods of presentation do not produce images at the correct focal distance from the viewer's eye. For most flight conditions, it is perfectly acceptable to have all images at infinity (or at a fixed distance if a projection screen is used). However for simulation of the view in close proximity to the ground the pilot's ability to judge the distance of near field objects is significantly reduced, because he is denied the use of binocular

cues. It is slightly disturbing to await take-off in the cockpit of a fighter simulator, and to see the runway beneath the aircraft at infinity, rather than a few feet away. This sensation is less troublesome in the airliner simulators, because of the greater distance of the eye to the runway. Nor does this deficiency seem to be a critical factor in the representation of the final stages of landing, or of ground roll, since nowhere in the literature is mention made of its intrusion.

The visual display requirements are task-dependent, and will therefore be discussed under the broad headings of taxiing, ground roll, and landing flare, with the obvious proviso that a particular application as listed in Section 2.0 may have associated with it a special display requirement.

4.1.2 Taxiing

The representation of a task more difficult than steering in a straight line makes considerable demands on the visual system. 'Seeing into a turn' is clearly important, so that a wide field of view is essential (figure 9). Three window systems cater reasonably well for the azimuth field of view, but are barely sufficient for the view in elevation, since the pilot will use head movement to increase the downward view from the cockpit. The important cases of taxiing in close proximity to other aircraft and buildings, including the docking case, make it necessary to generate considerable scene complexity, including markings/lights on runways and buildings, and other marshalling aids. Fortunately, the numbers of objects involved is not large, and the changes to the visual scene do not occur in a rapid manner. Consequently, current visual systems are capable of creating the images needed for this phase of flight.

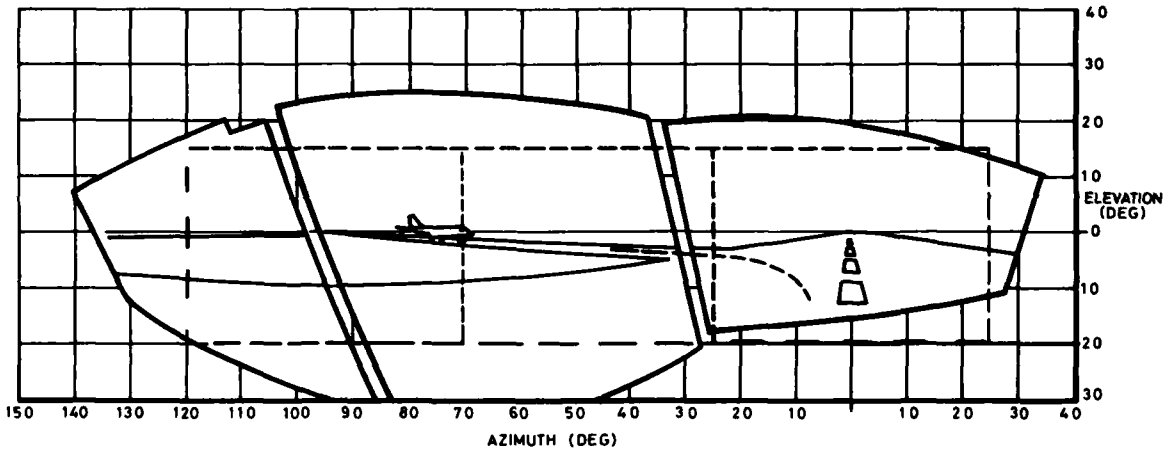

Figure 9 Three window CGI on B.737 vision envelope

4.1.3 Ground-Roll

Having taxied into a take-off position, the visual display requirements change in emphasis. For take-off, the pilot is primarily concerned with the view directly ahead, and although a wide field of view will contribute to the realism, successful simulation of take-off and landing ground roll is possible with a field of view restricted to around 50^{o} x 30^{o}. Tunnelling of vision with increasing speed close to the ground occurs and the illusion of speed has to be created. The visual system is the major contributor to the illusion largely through textural quality (the granularity of the runway surface), supported by correct representation of scaled objects such as runway markings and lights. The scaled objects also play a vital part in giving to the pilot the appreciation of distance - particularly important for ground handling.

The dynamic response of the display, particularly at small amplitudes, becomes important in the ground roll. During take-off and landing the pilot can see the dynamic response of the airframe/undercarriage following brake application or release. Wind and runway roughness also cause excitation of these modes. The pilot must also be able to resolve on the display the small heading changes needed for accurate steering, and to differentiate between heading and drift. For rotation and lift-off, the pilot must get an accurate appreciation of pitch attitude from the visual system.

4.1.4 Landing Flare

The behaviour of an aircraft post-touchdown is pre-conditioned by events a few seconds before touchdown. A short discussion is therefore useful on the simulation aspects of the landing flare, since if the simulator does not represent the flare manoeuvre sufficiently well, aspects of control following touchdown (use of thrust reversers, behaviour in cross-wind) will be compromised.

In general, flight simulators do not represent the flare manoeuvre very well. Standards are improving, as better display systems are introduced, and as the aircraft models become more accurate. Even so, large differences in performance between simulator and flight are usually present, and will be discussed later. The problem of simulating the landing flare varies with the type of aircraft - a distinction is drawn in reference 11 between large and small aircraft. The visual requirements for the representation of the landing of the large aircraft are considerably eased by the relatively large distance of the pilot's eye from the runway; additionally, the pilots task during the landing flare is generally less demanding in the large aircraft than in the small one. Consequently, many examples can be found where success has been achieved in simulating the landing flare. Evidence of this success is seen in the widespread use by air carriers of simulators which meet the FAA Regulations to allow type conversion to be made without the need for in-flight training.

The features of the visual display which contribute to this success are difficult to isolate. A wide field of view is desireable; some pilots would say essential, because of the value of peripheral cues in judging the last few feet. Good display resolution is also important, because the correct estimation of range to touchdown is vital, together with an accurate appreciation of aircraft attitude. CGI systems are superior to camera/model systems in these respects, but suffer with respect to scene detail. The recognition of this latter deficiency has led to the introduction of textural patterns on runway surface elements, with a consequent improvement both in the subjective impression of the landing flare, and in the achieved performance. Unfortunately very few controlled experiments to quantify these improvements have been made.

4.2 Motion Systems

4.2.1 General Remarks

In a ground based simulator it is impossible to reproduce all the linear and rotational accelerations experienced by a pilot in flight. The size of the building containing the simulator and the power required to drive the motion platform eventually impose restrictions. However, depending on the regime of flight and the pilot's task circumstances arise in which it is possible to give the pilot a reasonable representation of the motions which would be experienced in flight.

The value of providing such cues for training of USAF pilots has been questioned, however. In reference 13, experimental evidence is quoted to show that pilot training for single-engined jet aircraft is just as effective without the motion cues in the simulator as with them. Consequently, the procurement policy of the U.S. Air Force was changed to reflect this apparent lack of cost/effectiveness of motion systems, and to put greater emphasis on visual cues. The USAF lack of faith in motion cueing is not reflected in the FAA Regulations for Approval of Aircraft Simulators; for Phase I training, a three axis motion system is mandatory, and for Phases II and III, a motion system which provides motion cues equal to or better than those provided by a six-axis motion system is called for (Reference 14). Also the concensus of pilot opinion, both civil and military, favours the use of motion system in training (Appendix C in reference 15).

Research simulators have also highlighted differences in pilot performance, with and without motion cues. The differences are exaggerated if the stability of the vehicle in question is low, but even in the case of aircraft ground handling, differences in performance with and without cockpit motion were identified in a NASA Langley study of lateral steering following engine cuts (Reference 16). In this case, the motion cues were such as to assist the pilot in his control task, either by triggering an early response to engine failure, or by providing an additional sensory cue to help stabilize the control loop. Figure 10, from reference 16, shows that the pilots were able to reduce lateral deviations due to engine-cut by at least 30 per cent.

The other influence of motion cues is to add to the pilot's difficulties, by providing the disturbances and jolts which occur in flight due to turbulence, airframe buffet, or ground contact. In general, these disturbances are at higher frequency, and are easier to represent because of the smaller excursions required of the motion system. Moreover, errors in amplitude and phasing are acceptable, since they are outside the range of control by the pilot. There can be little doubt that such cues add greatly to the realism of the simulation.

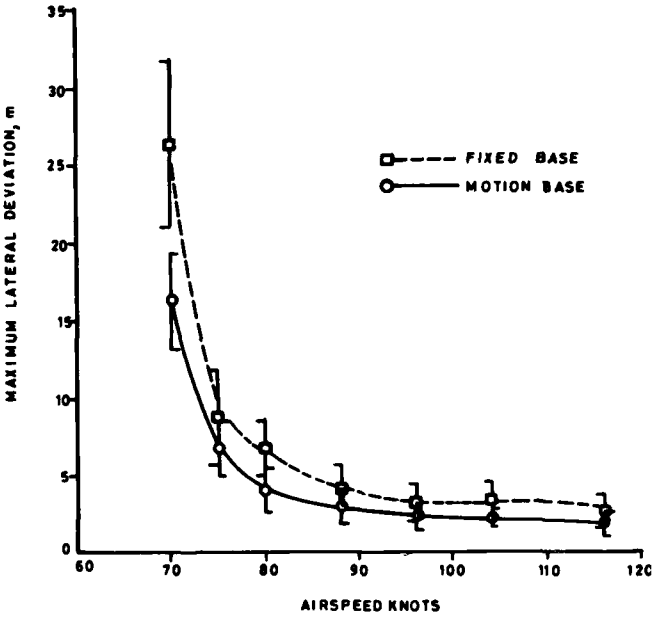

Figure 10 Effect of engine-cut speed on the lateral deviation on the runway of a 737-100 simulator

4.2.2 The Need for Motion Cues in Ground-Roll

Later in this report, examples of successful research programmes concerned with ground-roll will be presented. In some cases motion cues were given, in others, the simulation was fixed-base. In the latter cases, it is unlikely that the missing motion cues would have influenced the pilot's assessment - the evaluation pilot's job is to take account of the simulator shortcomings, be it in cockpit furnishings, motion system, or visual display. Each case must be looked at on its merits - for example, a study of vibrations in the cockpit due to runway roughness needs a motion system, whereas a study of stopping distance with various retarding devices probably would not. In all cases, however, the inclusion of motion would add to the realism.

Pilots in training simulators are not expected to make such large extrapolations to flight as test pilots in a research simulator. In both situations, however, it is essential for the pilot to establish unequivocably whether or not the aircraft is on the ground. In this repect, the motion system is a great help. Anyone who has sat on the flight deck of a large airline simulator, with a night-dusk visual and six-axis motion system, and has seen the representation of take-off, from brakes-off to climb-out, will subscribe to the realism of modern flight simulators. The noise and vibration of engine run-up, the dipping of the nose as brakes are released, the visual sensation of this massive thing beginning to move, and the forward acceleration provided by the motion system all contribute. Nose wheel and mainwheel unstick are unmistakeable, and the structural resonances and change in buffet level associated with undercarriage and flap operation are faithfully reproduced. The motion system plays a substantial part in creating the illusion.

The requirements for a flight simulator in research on the design of the flight deck of advanced transport aircraft are discussed in reference 17. A motion system is said to be needed to improve the representation of push-back (from the gate), brake release, and vibration during taxi.

4.3 Cockpit Cueing

Additional methods of providing the sensation of movement are available. Cockpit vibration can be produced by mounting small electrical or hydraulic devices between the cockpit and the motion system. Alternatively, the seat itself can be mounted on a shaker, to reproduce buffet effects and other airframe resonances.

These devices are particularly useful in the simulation of ground handling. As stated previously, knowledge of ground contact is all-important to the pilot, and the transmission of this information comes partly through airframe vibration. Low amplitude, high frequency actuators are a cost-effective way of producing these sensations, rather than using a full six axis motion system.

Noise is also a cheap and rewarding way of adding to the realism. Again, a greater range of noise cues occur on the ground than in flight. Typical sources are undercarriage rumble, tyre squeals, brake operation, reverse thrust operation, air-conditioning, aerodynamic noise, flap motor operation, and engine start/stop (Reference 17).

Some of these cues provide feedback to the pilot to influence his performance in the control task. Others add to the realism, or 'face-validity' of the simulator. This latter aspect is particularly important in the training application, but it should not be dismissed in research simulators as making no contribution to the experiment. The realism of a simulator is a subjective matter, so that factors which help to provide realism will not necessarily prove their worth when examined in a quantitative manner.

A further cueing device is provided by cockpit illumination. Air combat simulators use 'g' dimming of cockpit lights and displays to represent normal acceleration. Similarly, the impression of forward motion during ground roll could be augmented by moving shadows in the pilot's peripheral view, to represent variations in reflected external light. Lighting effects associated with atmospheric conditions are required in Training Simulators to meet the criteria for FAA Category III Certification. They must be co-ordinated with any associated cockpit motions - for example jolts in a thunderstorm.

4.4 Modelling/Software

The key to successful simulation is to achieve an accurate dynamic model of the aircraft, subjected to control inputs, ground restraint, and atmospheric influences. The equations of motion required for such a model and the data sets to implement them in the model were discussed in section 3.2. The choice of computer to solve these equations is critical.

In the early 1960's, attempts to represent an aircraft on the ground used analog computers (reference 18). Even with large machines, comprising several hundred amplifiers, function generators, multipliers, and the like, ingenuity was needed to contain the problem within the computing capacity available. Difficulties also arose due to scaling, static accuracy of components, and drift. Dynamic response requirements at high frequency were easily met but it was something of a triumph when, at low speed, the sum of the calculated loads on each of the wheels was found to equal the weight of the aircraft. Early efforts were also hampered by the need to use rigorous checks to detect component failures, and to obtain repeatability from day to day. Even so, useful insights were made in the areas of aircraft ground handling and dynamic response.

The greater reliability, capacity and accuracy of digital computers have transformed the modelling problem. For several years, analog computing elements were retained in the loop, to deal with the high natural frequencies associated with the dynamics of the undercarriage. The relatively slow speed and small memories of the the early digital computers limited their use in 'real time' applications of large bandwidth. The weakness of hybrid computation however, lay in the transfer of data between analog and digital. The time taken to transfer data back and forth slows down the digital computation, and the overall accuracy is determined by the accuracy of A to D and D to A conversion.

Even with "all digital" computing, the solution of the equations of Appendix B calls for special care. In real time applications, computer programmes are structured according to a cycle time pyramid, such that not all equations are updated at the same rate. Parameters which vary slowly, such as Mach Number or height get low priority, whereas the dynamic inputs are dealt with at the maximum rate. It is often considered that 50 Hz is a suitable minimum update rate.

A full representation of a small high performance aircraft is likely to call for faster rates. Rather than use a much larger, more costly digital computer, the way in which this requirement can be met is to chose a suitable system architecture. Such a system is described in reference 19. The role of the analog computer in the hybrid computation referred to earlier is taken by Array Processors (AP), to represent the aircraft, the flight control system, and the undercarriage. The AP is a peripheral processor, under the control of a small host computer. To use APs in this way, a high level language compiler is essential for ease of programming and validation. The system described can handle data update rates at the peak of the cycle time pyramid in excess of 250 Hz.

5. Simulator Effectiveness

The best illustration of the capability of flight simulators to represent aircraft handling on and close to the ground is to give specific examples of their use. The examples are in two categories, Research and Development, and Pilot Training. Like most attempts at categorisation, the pegs do not always fit in the holes; nor can all the examples be fully referenced. They do illustrate, however, the diversity of the problems which can be investigated in this way.

5.1 Research and Development

5.1.1 F-4 Aircraft Study (Reference 20)

Aircraft ground handling operational safety margins are compromised by inadequate braking and/or directional control capability resulting from combinations of such factors as slippery runways, crosswinds, extended touchdown points, excessive velocity, and possible equipment malfunction. Past research and development efforts using instrumented test aircraft have concentrated on defining the braking problem while, because of safety constraints, the directional control aspect has remained essentially unexplored. To help remedy this lack of available data, researchers at NASA Langley initiated a feasibility study in 1973 with McDonnell Aircraft Company to expand current flight simulation capability to include the complex interactions between the runway and the landing gear system. An F-4 was selected as the baseline aircraft for this effort, described in reference 20, because of landing gear model simplicity (single wheels) and extensive parameter data available on this aircraft including tire/runway friction performance measured during both flight tests and Langley track tests for a variety of runway surface conditions. Pilots demonstration and validation runs were conducted using a five-degree-of-freedom (lacking longitudinal surge) motion based simulator and an F-4 cockpit equipped with a dual raster/stroke cathode ray tube visual display system providing an out-the-window 45 degree forward field of view and stereo speakers for sound cues of engine rpm, aircraft tire touchdown, antiskid brake control cycling, and runway rumble. Five pilots participated in performing 183 simulated landings on dry, wet, flooded, and icy runway conditions. Their comments on the ground handling phase of the simulation were generally favorable and good aircraft stopping distance correlation was obtained between simulator and actual flight test data. Adding longitudinal motion to the simulator, including runway crown and roughness in software modeling (simulated smooth, flat runway in this study), and enhancing the visual display system with color and a larger field of view were recommended modifications to improve simulation fidelity.

5.1.2 DC-9 Aircraft Study (reference 21, 22 & 23)

Based on the encouraging F-4 aircraft simulation results, NASA Langley implemented follow-on contractual efforts first at McDonnell Aircraft Company (see reference 21) and subsequently at Douglas Aircraft Company (see reference 22) facilities. These studies extended the aircraft ground handling simulation capability to include a DC-9, Series 10 jet transport and provided evaluation data on further refinements to both software and hardware components of the simulation. Effects of runway crown (cross slope) and roughness (longitudinal profile) together with engine thrust reversers were added to the software models which included steady, as well as gusty, crosswind conditions. Several different patchy friction surface conditions corresponding to runway ponding and localized ice patches were also defined for use in both digital (preprogrammed tire drag and side force coefficients) and an analog (included actual wheel/brake hydraulic system hardware) antiskid brake system model. The visual display system, which included a computer controlled television camera directed at a large airport-runway-terrain model (scale: 750 to 1) to provide pilot's eye level view on color monitors positioned at the simulator cockpit windscreen, presented an angular field of view of 48 degrees horizontal ($\pm$24 degrees) and 36 degrees vertical (+16 degrees; -20 degrees).

In evaluating the DC-9 aircraft ground handling simulation capability developed during the Douglas Aircraft Company effort, fourteen experienced pilots participated in over 800 checkout, validation, and demonstration runs. Good correlation was obtained between simulator and available flight test data. Qualitatively, most pilots considered the simulator performance realistic with good potential towards improving pilot training for operations under adverse runway conditions. The pilots all preferred motion over no motion for the simulation and they generally considered the digital antiskid brake system modelling better than the analog model for high friction surface conditions. However, on low friction surfaces, the analog model was preferred. In comparing various parameter time histories obtained during simulated aircraft landings on a variety of surface conditions with actual aircraft flight test data, the agreement shown indicated that the methods used in deriving the required tire/runway friction performance values for the simulation models were reasonable. Actual aircraft data, however, were not available to validate all the tire friction values used during the simulated aircraft landing, rollout, turnoff, and aborted takeoff operations conducted on a variety of runway surface conditions.

The DC-9 aircraft ground handling simulation capability has been implemented and validated at the NASA Langley simulator facility to provide a research tool for use in solving aircraft ground ooperational problems and conducting various parametric studies (see reference 23). NASA researchers are also continuing efforts to collect additional aircraft tire friction data required to define better simulation models and to identify improved computational techniques, based on empirically-derived relationships, for

estimating tire friction performance. These tasks may become more demanding and complex if the recent introduction of aircraft radial tires results in future widespread use. Several existing aircraft ground handling simulation models, including landing gear strut/tire dynamics, would require major modifications.

5.1.3 SAAB Viggen Aircraft

The engine thrust reverser fitted to SAAB's JA 37 aircraft is a very efficient device, adding greatly to the aircraft's landing performance. The change in lateral stability with thrust reverser is seen on figure 11. Thrust reverser development posed certain problems (reference 24) including the loss of an aircraft due to lack of directional control on the runway. The problem was solved not only by configurational changes to the thrust reverser, but also by changes to the nosewheel steering system to give improved directional stability. The work at SAAB was supported by more general investigations using a ground-based simulator at the Royal Institute of Technology (KTH) in Stockholm (reference 25).

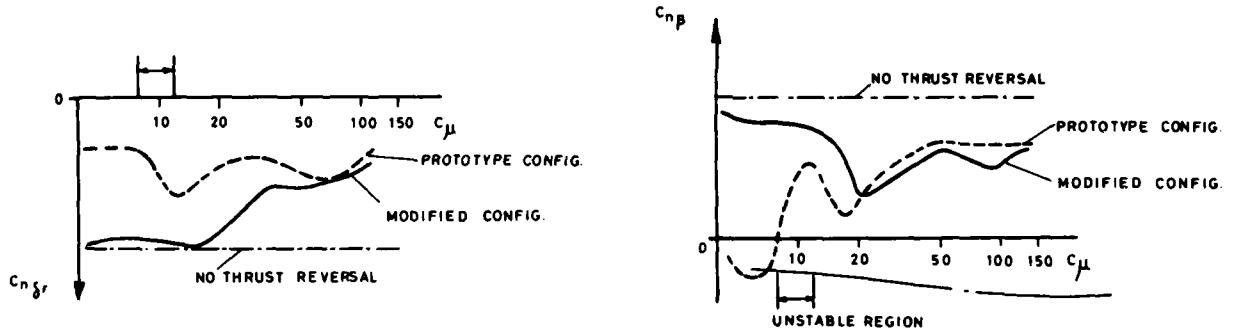

Effect on rudder power

Effect on static directional stability

Figure 11 Influence of Cμ, jet coefficient, on aerodynamic characteristics

This work is of interest, since it identifies six dynamic stability and control parameters which define handling in the ground-roll. The method is analogous to the traditional lateral handling qualities parameters (dutch roll frequency, damping, etc.) which have been studied extensively, in order to predict behaviour in normal flight. For example, the method would be useful to examine undercarriage layouts which differ from conventional main-wheels/nose wheel arrangements.

The simulation study at KTH was seen to confirm the actual JA 37 aircraft test findings and to give confidence that the proposed solutions were suitable for many varied conditions of runway surface and crosswind. The simulation model of the aircraft was reduced to two degrees of freedom (sideforce and yaw), on the assumption that for the configuration under test, the bank excursions were small (not true for narrow track, large oleo-travel landing gears). Because of this assumption, it was possible to use the roll axis of the simulator's motion platform to reproduce side-accelerations on the pilot.

5.1.4 Jaguar and Tornado Aircraft

The SEPECAT Jaguar aircraft is designed to have rough-field capability. Extensive use of computer modelling has been made to optimise the undercarriage design for energy absorption over rough surfaces, including runway repair matting. These techniques are in widespread use (reference 4) in non-real time application. Modern computers, which allow the models to run in real-time, give further insight into effects both on and from the pilot. In the former case, if the vertical motions are sufficiently violent they can interfere with the pilot's ability to apply directional control or braking; they can even transmit high frequency structural vibrations and so make the reading of instruments difficult. In the latter case, pilot inputs can easily aggravate or reduce critical loading conditions.

The PANAVIA Tornado aircraft development has used non-real-time mathematical modelling. Additionally, piloted simulations have been made by all three partner countries on the behaviour of the aircraft either on or in close proximity to the ground. Examples include studies at MBB of short take-off techniques, one of which identified control surface saturation/rate limiting as a potential source of trouble, until flight control changes were made.

The Tornado thrust reverser development benefitted from the earlier Viggen experience in Sweden, simulator studies were made at B.Ae., MBB and Aeritalia of directional control during ground roll. The prime responsibility for ground handling simulation was with Aeritalia, and the support to flight test for the clearance of configurations under varying runway and crosswind conditions was done there.

More recently, the clearance of high weight take-off configurations has been assisted by flight simulations, concurrent with flight testing. Performance demonstration of this type calls for accurate modelling, particularly with respect to the engines and the brakes. Once the accuracy of the simulator is established, considerable benefits accrue. In particular pilots are happy to prepare for flight testing in the simulator, and to establish the margins of the more critical cases, such as engine malfunction during the take-off run. Unstick speeds are accurate to within ±1 knot, and unstick distances to within a few metres, but this level of accuracy is only possible when a good data base has been established.

5.1.5 Landing Flare

There have not been many attempts to investigate the difficulties of simulating the landing flare manoeuvre. The landing flare has, however, been included in many trials to investigate other aspects of aircraft design or operation, in which completion of the landing, including ground roll, is required. Consequently, much evidence is available to show that both subjectively and quantitatively, there are significant differences between simulation and flight. Mean sink rate at touchdown is a useful parameter with which to compare performance measured from flight and from simulators. Table 2, from reference 26, gives such a comparison. Whereas sink rates at touchdown from flight measurements are Between 0.2 and 0.6 m/s, the best simulator results are never less than 1.0 m/s. Moreover, the reporting of these trials clearly indicates that the simulator results depend on both the simulator and on the experience of the pilots in the simulator.

Table 2 Mean sink rate at touchdown

Aircraft	Flight/ Simulator	Visual Display	Type of Landing	No. of Pilots	Mean Sink Rate m/s	Standard Deviation
Comet	Flight		flare	4	0.26	0.21
"	Simulator	TV model	flare	7	1.28	0.84
VC 10	"	"	flare	7	2.07	1.10
"	"	"	flare	5	2.0	-
Jet Transport	Flight		flare	20	0.46	-
" "	Simulator	early TV	flare	3	2.60	-
" "	"	"	flare	20	4.81	-
'good' aircraft	Simulator	CGI	flare	8	1.35	-
" "	"	TV model	flare	8	1.7	-
" "	Flight		flare	-	0.3 - 0.6	
Sea Vixen	Flight		no flare	2	2.16	0.49
"	"		guided flare	2	0.79	0.26
"	"		flare	2	0.55	0.275
SAAB 105	Simulator	CGI	no flare	5	2.22	0.42
"	"	CGI	director	5	1.09	0.39
"	"	CGI	indicator	5	1.03	0.40
"	"	CGI	flare	5	1.29	0.33
"	"	CGI	with lags	5	1.64	0.95

Sink rate data can also be presented as a sink rate probability curve - the probability of the sink rate at touchdown exceeding a particular value. Figure 12 again compares simulators with flight test results on this basis. Again, it is clear that the performance in the simulators does not match that achieved in flight. In fairness, the worst simulator results are from elderly simulators, now retired.

Reference 26 describes an investigation in which the SAAB 105, a small trainer aircraft, was simulated and landing performance was correlated with pilot opinion. Guided (by flight director) and unguided landings were simulated, and the visual display (single window CGI) was degraded for some trials by introducing lags in the display. Without lags, good performance was achieved; introducing lags ruined performance (figure 13), without further degradation in the pilot ratings.

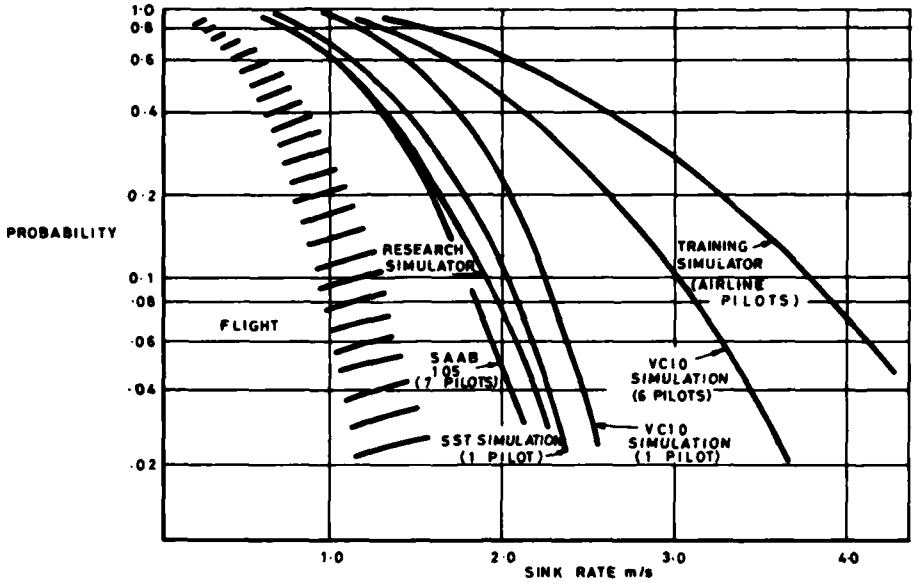

Figure 12 Landing performance in simulators (from Ref.26)

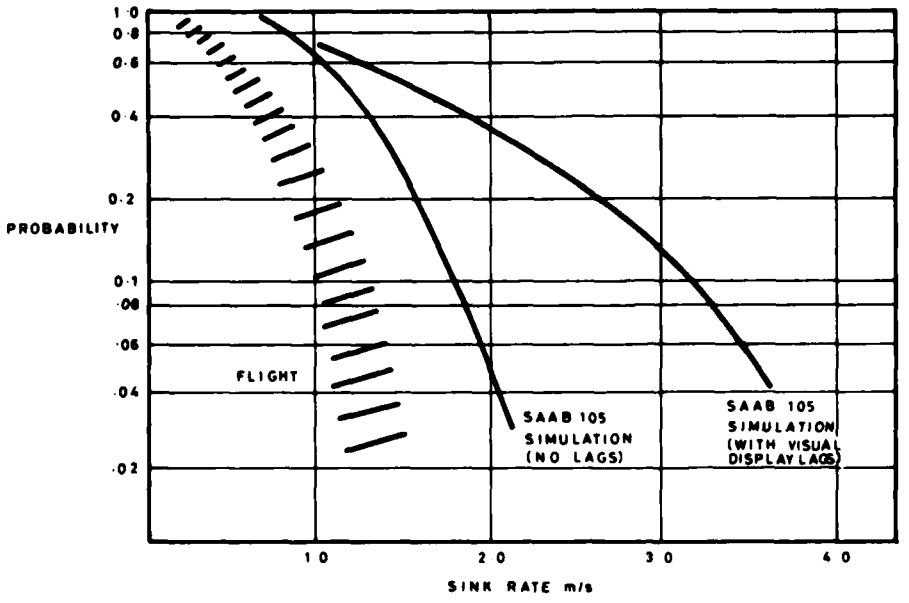

Figure 13 Effect of display lags on touchdown performance (1)

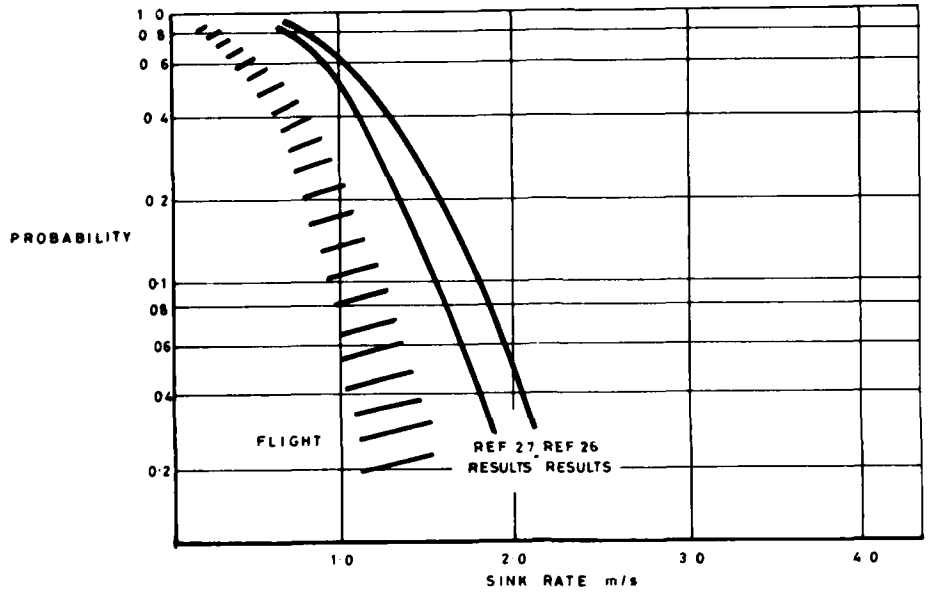

Figure 14 Effect of display lags on touchdown performance (2)

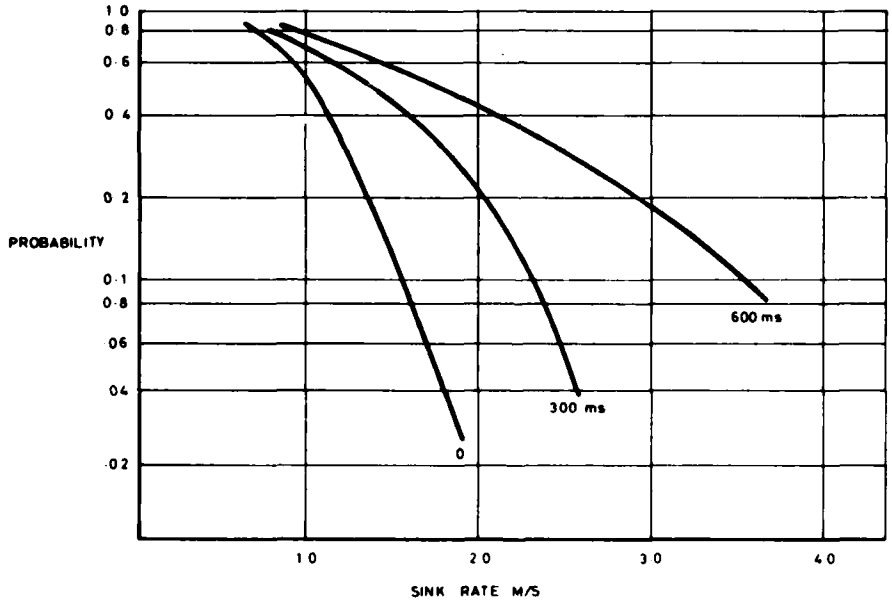

Figure 15 Effect of time delay in display on touchdown performance (Ref.27)

A follow-on study (reference 27) confirmed the previous conclusions, that static and dynamic accuracy in the visual display is essential to achieve good touch-down performance. Also, an accurate model of aerodynamic ground-effects is needed. The comparison between the touchdown performance achieved in the two experiments is seen on figure 14. The slightly better performance in the second experiment is possibly due to a combination of an improved ground effect model and a small reduction in the pitch sensitivity of the simulated aircraft.

The effect of a time delay on signals to the visual display was investigated in the follow-on experiment. Time delays up to 150 ms had negligible effect on pilot opinion or performance, but greater time delays had progressively more serious effects on performance. The probability of touching down with a sink rate of more than 1.5 m/s was increased from 1 in 10 landings to 1 in 3 landings, when a 300 ms time delay was introduced (figure 15).

One aspect of these (and other) experiments on touchdown performance is the scatter in results between individual pilots. The scatter is hidden when mean values are taken, and when 'best curves' are drawn on a probability plot. One consequence is that to obtain credible results from a simulator trial, many more runs are required. More serious, however, is the conclusion that with the standards so far achieved in research simulators, only a percentage of pilots get near to reproducing their "in flight" performance in the simulator.

5.1.6 Other Examples

Take-off performance can sometimes be limited by the balance of forces needed to lift the nosewheel and rotate the aircraft. In the past static calculation of the moments has not given an accurate prediction of the nosewheel lifting speed of many aircraft. In one or two cases, unnecessary design features were introduced to offset the performance loss due to a high predicted nosewheel lifting speed. Flight simulation of the take-off has allowed dynamic considerations to be introduced. They can significantly reduce the nosewheel lifting speed of aircraft with good acceleration capability in take-off. In particular, it can be demonstrated that the nose-oleo can act as an energy storage device when compressed, and be used to assist the elevator to raise the nose. The amplitude and phasing of the pilot's input also influences this particular manoevure.

A second, more specific example where simulation can assist in aircraft development is in the detailed undercarriage design. Severe airframe vibrations were experienced on landing during the early flights of the TSR-2 (a prototype strike aircraft, which flew in 1965). The capability to represent the undercarriage linkage, stiffnesses, damping and aircraft structural characteristics is well within the range of computing now used for research and development simulators, and would identify a problem of this type before flight.

Mention should also be made of the assistance which the simulator can give to the design of VTOL aircraft, helicopters and hovercraft, when operating in contact with, or close to the ground. In addition to modelling requirements discussed previously, more attention to representing airflow in ground effect is necessary. Once the model is established, a wide range of problems associated with operation on or close to the ground can be solved on the simulator.

5.2 Pilot Training

5.2.1 FAA Transition, Upgrade, and Total Crew Training

The Federal Aviation Administration (FAA) first introduced rules governing the use of simulators for crew training in 1980 and issued an updated Advisory Circular in 1983 (reference 14). When first proposed, they were regarded in some quarters as a bold step, since training which had previously only been possible in the air could now be done on the ground, provided that the simulator in question met certain requirements. Three levels or phases of simulator capability were described and the requirements for each phase, labelled I, II and III were defined.

In particular, a simulator meeting the requirements for Phase II allows transition and upgrade training, and checking to be done. Transition training is the training required for a pilot to move from one airplane to another in the same group, e.g. B 707 to B 727. Upgrade training is a change in pilot qualification, e.g. copilot to captain. Phase III is designed to allow all but static airplane training, the line check, and operational line experience to be conducted in the simulator.

The Phase II requirements relating to ground roll include representative stopping and directional control forces for at least the following runway conditions: dry, wet, icy, patchy wet, patchy icy, wet on rubber-residue in touchdown area, representative brake and tyre failure dynamics (including anti-skid) and decreased brake efficiency due to high brake temperatures. The Phase II visual requirements are for a dusk/night system, 75^{o} x 30^{o} field of view, and cloud/patchy cloud, fog/patchy fog effects. Also needed is the capability to represent ground and air hazards such as another airplane crossing the active runway or converging airborne traffic. A motion system capability with six degrees of freedom is also specified for Phase II simulators.

The Phase III requirements call for, in addition, better modelling of the aircraft and the atmosphere, and noises co-ordinated with visual weather effects (e.g. precipitation). The visual system requirements add to Phase II the need for daylight, more scene content, and 3 arc minutes resolution. Special effects include landing over water, runway gradient, thunderstorms and snow covered runway.

Manufacturers and operators have responded to the challenge set by the FAA. The incentive to use simulators rather than aircraft is contained in a 1980 FAA statement supporting the new regulations: "....the Faa estimates that over $67 million per year could be saved by the U.S. Air Carriers in fuel costs and $25 million in operating costs if the industry fully implements the advanced simulation plan. In addition, economic benefits will result to the public and the operator by having additional airplanes available that would otherwise be committed to training".

By February 1984, 36 Phase II simulators and 2 Phase III simulators were operational. Ground roll simulation has therefore become a routine matter for a certain class of aircraft, and pilot comments on the fidelity of Phase II and III simulators is very favourable. The emphasis on fidelity of aircraft ground performance requires specific tests to be carried out by the aircraft manufactur- er, to provide a full and accurate data-set to the users. An example of such tests is seen in reference 28, which relates to the lateral steering of the B 727 on the ground. The savings in training costs fully justifies the expense of this additional testing.

Equally important in meeting Phase II and Phase III simulator standards is the availability of data relating to wheels and tyres in contact with the runway surface, as discussed earlier. Measurements on different types of surface, under different conditions, provide the data base, so that the aircraft behaviour on the ground can be made to conform to that experienced by a specified aircraft, at a specified airport, under specified weather conditions.

5.2.2 NASA-Shuttle Orbiter

The NASA space programme in general, and the Shuttle programme in particular, is an excellent example of the use of flight simulation for pilot training. The Orbiter in its recovery mode is an aircraft which calls for special skills from the pilot. It is a one-shot operation, in a vehicle where the primary design considerations of its role in space have led to severely compromised aerodynamic flight performance. The weight distribution in the fuselage gives high inertia in pitch; the aerodynamic surfaces to produce lift and pitching moment are not as effective as in more conventional aircraft. Additionally, control actuator sizing is based on more severe weight, volume and power restrictions than would apply to conventional aircraft. Rate-limiting and saturation is more likely to occur. For similar reasons, the Shuttle undercarriage is not be designed to withstand exceptionally high loads at touchdown. Nevertheless, accurate and repeatable landings are now a routine matter - an achievement which is perhaps overshadowed by the dramatic happenings in space. Simulation has played an essential part, and will continue to do so.

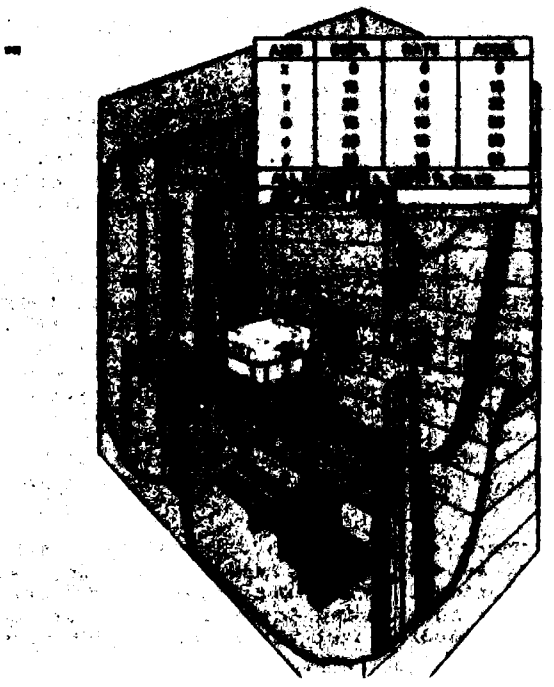

Figure 16 Vertical motion simulator, NASA Ames

One such simulation is performed on the large VMS (Vertical Motion System) at NASA Ames. A typical investigation (running in mid-1983) concerns recovery to Senegal, following early abort of the mission. The runway length at Senegal, West Africa, is not generous for the Shuttle, which approaches in a 20^{o} glide, at a speed of 285 knots. The flare is initiated at 2000 feet, and touchdown occurs at around 185 knots.

The simulation of this recovery is most impressive. In addition to the motion system, a Link CGI visual system presents the view of the runway and surrounding country from 5000 feet to touchdown. The flight controls, instruments and head-up display are representative of the Shuttle, and the various modes of operation (fully manual, assisted, or fully automatic) can be selected. Visibility can be varied; so can the wind and the turbulence level.

Astronauts confirm the realism of the simulation, and regard it as an essential preliminary to Shuttle operations. Not only does the pilot achieve complete familiarity with the handling of the Shuttle under all circumstances of operation, including degradation due to failures or atmospheric conditions; he also builds up confidence that all eventualities are within the scope of man and machine.

Several aspects of this simulation are relevant to a discussion of ground-roll representation. The astronaut's task is to achieve a touchdown at low sink rate at a prescribed point on the runway and, after touchdown, to reduce speed by aerodynamic and wheel braking and to keep directional control. The measure of success achieved in the ground roll phase depends critically on how well the flare manoeuvre has been performed. Conversely an investigation of flare technique would lose value if the simulation neglected to represent post-touchdown tasks.

The large amplitude motion system makes a valuable contribution to the realism of the simulation. Since the flight path of the Shuttle is largely pre-determined as the touchdown point is reached, the wash-out terms in the drive laws can be gradually reduced during the approach. The large travel available allows 1 to 1 motion below 100 feet simulated height, so that arguments about the realism of the motion disappear. Ground awareness is acute; if the landing is heavy, the pilot gets instant feedback. He also feels the 'rumble' of the main wheel support. As speed reduces, and the nose drops, nosewheel contact is felt as a judder, augmenting the large attitude change sensed through the pitch motion, and seen on the visual display.

The visual system is also well suited to the task. The initial flare manoeuvre cannot be judged by visual reference to the ground - the pilot uses the flight director with confirmation from the chase aircraft. As the flare continues, lateral and vertical deviations, cross-wind effects, and distance to touchdown are accurately presented. The eye-height at touchdown is 35 feet, which reduces the need for fine textural detail on the runway.

5.2.3 Airline Transition Training

As discussed in section 5.2.1, reservations were expressed from several quarters when FAA Regulations were introduced which allowed pilots to qualify on simulators alone for route flying on a new type of transport aircraft - the so called zero/zero conversion. One of the doubts was whether the technology of flight simulation was sufficiently advanced to meet the standards required by the FAA, in FAR 121, Appendix H.

To meet such comments, a study was carried out in 1980 on the B 727 and DC 10 simulators used for pilot training by United Airlines. The study was intended to compare directly the performance in the landing manoeuvre of airline pilots converting to the B727 and the DC 10 in both the aircraft and the flight simulator, and is reported in reference 29. Further analysis of the results relating to the DC 10 is reported in reference 30.

Forty-eight trainees were used for the B 727 study, and eighty-seven trainees for the DC 10 study; the results therefore are highly significant. Also, the work is unique in producing quantitative data from a training environment, using airline pilots. A detailed discussion of the results is outside the scope of this paper, but one or two points relevant to the landing flare are noteworthy. Figure 16, from reference 29, shows the measured sink rate at touchdown from flight and simulator, plotted against the time from flare initiation to touchdown. "The figure indicates a rather good correspondence between the distribution of landings in the simulator and aircraft; but both have large variances" says the report. "The large spread of scores may have been due to the inexperience of the trainees in the 'new' aircraft". The larger overall mean sink rate in the simulator than in the aircraft is a familiar trend. The solid lines show mean sink rate as a function of Δt. The "simulator" and "aircraft" lines only diverge for values of Δt greater than 5 seconds. A flare time of more than 8 seconds indicates either too high a speed during the flare, or an early initiation of the flare, resulting in a 'floater'. Visual display limits often cause inexperienced pilots to "balloon" in the simulator, perhaps accounting for the trend of increasing sink rate for Δt greater than 8 seconds.

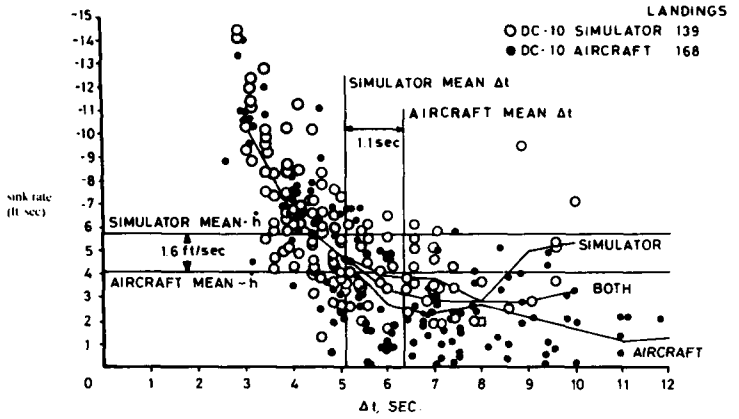

Figure 17 Relationship between sink rate ($\dot{h}$) and time interval (Δt) from flare initiation to touchdown

Reference 29 comments on the range of performance which was recorded. It is worth noting that most of the real landings were made at night, and that the visual display on the simulator was a single window Novoview - a night CGI system. The comment is made that the pilots who had high sink rates in the simulator also had high sink rates in flight, suggesting a good correspondance of task.

The data presented in reference 30 allow a sink rate probability curve to be drawn for comparison with the work discussed in section 5.1.5. The curves are given in figure 17, and illustrate the complexity of comparing flight and simulator data from various sources. The DC 10 results were obtained in special circumstances (pilots new to the aircraft, night landings). The scatter seen in the flight results must reduce with experience on the aircraft; otherwise, there would be a need to review the design stressing case for civil aircraft undercarriages. It would be encouraging to confirm that performance in the simulator is better, if pilots experience on the aircraft are used. Reference 30 suggests, however, that flare technique used in the simulator differs in some respects to that used in flight. "There is evidence that the inferior simulator technique carries over into at least the first few actual landings, if the pilot has trained solely in the simulator."

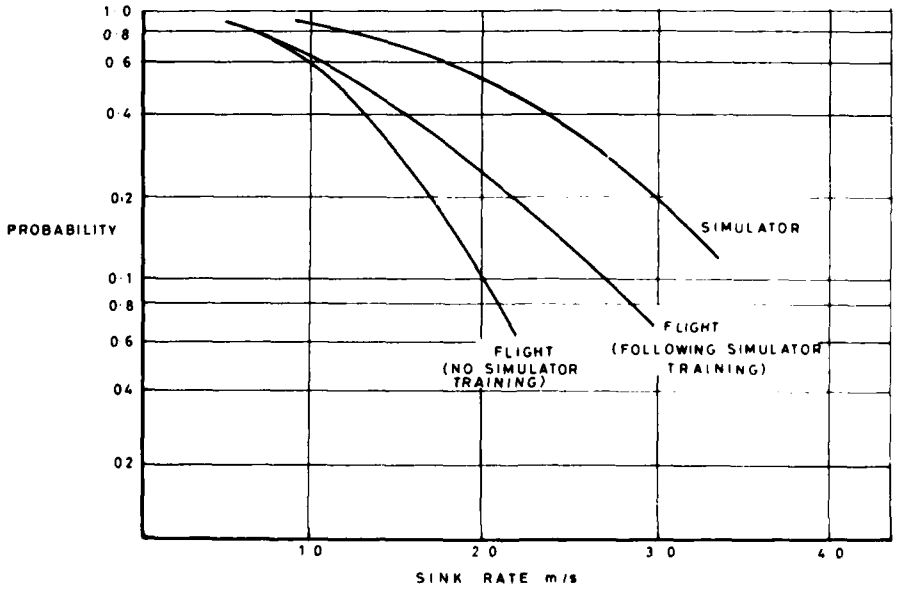

Figure 18 Airline landing flare data comparison: flight vs simulator

6.0 Conclusions and Recommendations

6.1 Conclusions

1. A full representation of the behaviour of an aircraft during ground roll makes considerable demands on current standards of simulation technology. Once achieved, however, the utility of the simulation covers an extremely broad field. The applications fall conveniently into two categories - Aircraft Research and Development and Pilot Training.

2. Use has been, and is made of simulators in both of these catagories. Several examples are presented, to illustrate the diversity of problems which have been studied in this way. Most of these simulations had minor deficiencies, which did not deter from the value of the investigation. They indicate the direction to take, as better hardware or techniques become available, to improve the standards of ground roll simulation, and to extend their scope. The examples also show the features of the simulation which are important to achieve pilot acceptance.

3. Section 2 lists the wide range of operations on or close to the ground which are potentially within the scope of ground-based simulators.

   On the research and development side, much of the benefit is related to performance prediction and demonstration, for both civil and military aircraft. The mandatory requirements set for the design and clearance of civil and military aircraft lead to extended and extensive testing. The flight simulator is able to reduce both the cost of, and time taken in performing some of these tests, once a satisfactory standard is available.

   On the training side, the items in section 2 put an emphasis on safety of operation. Many conditions which are rarely encountered by pilots (such as extreme combinations of atmospheric conditions, runway surface, and aircraft operating state) can be experienced in the simulator, giving the crew the confidence to deal with all situations which might arise.

4. The basis of a successful simulation of ground-roll lies in the mathematical model which represents the component elements and the inter-action between them. Appendix B contains a comprehensive set of equations; simplification of these equations is possible, when the model is tailored to the specific requirements of the simulation. The behaviour of the aircraft on the ground is greatly influenced by the forces generated between the tyres and the runway, and the transmission of these forces through the landing gear to the airframe. The methods of measuring and describing these forces have been presented.

5. The main hardware elements of flight simulation, cockpit and controls, visual system, and motion system, have been discussed. The contribution of each of these items varies with role of the simulator and its application. The cockpit and controls should be as representative of the actual aircraft as possible. The use of a motion system is strongly recommended, for improved realism and pilot acceptance. Visual requirements vary with task. A multi-window CGI system with ground texture is adequate for most applications.

6. Greater use could be made of flight simulators in research and development of aircraft behaviour on the ground. Modern computers can easily deal with the required mathematical models, allowing performance and handling to be studied.

7. The FAA Phase II and Phase III simulators for pilot training call for good ground-roll simulation. This report, and the recommendations which emerge, give guidance on how to meet these standards.

8. Wider acceptance of ground roll simulation will require greater standardisation of the modelling and validation processes. Equations of motion and response criteria to define aircraft behaviour when airborne are widely accepted. The ground-borne equations have received less attention, notations vary, and criteria for acceptance are not fully established.

6.2 Recommendations

The following recommendations indicate the type of work which will fill in some of the gaps, and lead to further improvements in standards of ground roll simulation.

1. Good descriptions of runway surface conditions under all weather conditions, and the behaviour of tyres with varying load, speed and slip are essential. Efforts to provide such data should be expanded.

2. A range of mathematical models to represent ground behaviour should be developed, using a standard notation, together with a definition of the application of each model. Methods of validation (static and dynamic) should accompany each model.

3. All phases of ground operation need 'out of the window' visual cues. The usual reservations about current visual display systems apply - Is the field of view sufficient? Is higher resolution required? What benefit comes from texture and surface detail? Do time delays intrude? All these questions require investigation.

4. Post touchdown behaviour is pre-determined by the touchdown conditions, and work still remains to be done to improve landing flare simulation.

7.0 References

1. Proceedings, Interservice Industry Training Equipment Conference. "The Cost-Effectiveness of Military Training".
Jesse Orlansky, et al.
U.S. Institute of Defence Analysis. November 1982

2. R.Ae.S. Journal, "An Evaluation of Some Experimental Data on the Cost-Effectiveness of Flight Simulators".
Sqn. Ldr. C.G. Durose, R.A.F. March 1982

3. N.A.S.A. CR 1344 "Computer Mechanisation of Six Degree of Freedom - Flight Equations".
R.M. Howe, L.E. Fogarty May 1969

4. AGARD CP 326 "Aircraft Dynamic Response to Damaged and Repaired Runways".
52nd and 54th SMP Specialists Meetings April 1981, April 1982.

5. CEEDO-TR-78-39 "A Literature Search and Review of the Dynamics of Aircraft-Surface Interaction".
J.J. Cox, Jnr., W.M. Henghold, J.J. Russell
[U.S. Air Force Civil and Environmental Engineering Department office, Tyndall AFB] May 1978

6. NASA TR R-64 (Supercedes NACA TN 4100) Mechanical Properties of Pneumatic Tires with Special Reference to Modern Aircraft Tires. Smiley, Robert F.; and Horne, Walter B. 1960

7. NASA TN D-8332 Behaviour of Aircraft Antiskid Braking Systems on Dry and Wet Runway Surfaces - A Velocity-Rate-Controlled, Pressure-Bias-Modulated System. Stubbs, Sandy M.; and Tanner, John A. 1976

8. NASA TN D-4406 Review of Causes and Allevation of Low Tire Traction on Wet Runways. Horne, Walter B.; Yager, Thomas J.; and Taylor, Glenn R. 1968

9. NASA SP-416 Status Runway Slipperiness Research. Aircraft Safety and Operating Problems, Horne, Walter B. pp. 191-245. 1976,

10. AGARD AR 164 "Characteristics of Flight Simulator Visual Systems".
FMP Working Group 10. May 1981

11. AGARD CP 249 "Piloted Aircraft Environment Simulation Techniques". Paper 2 "Simulating the Visual Approach and Landing". A.G. Barnes
FMP Specialists Meeting April 1978

12. AGARD AG 248 "The Use of Simulators for Training In-Flight and Emergency Procedures".
E.E. Eddowes, Wayne L. Waag. June 1980

13. AFHRL-TR-79-51 "Training Effectiveness of Platform Motion: Review of Motion Research Involving the Advanced Simulator for Pilot Training and the Simulator for Air-to-Air Combat." E.L. Martin, USAF Human Resources Lab., Williams AFB, AE. February 1981.

14. Advisory Circular 121-40 "Aircraft Simulator and Visual System Evaluation ".
Dept. of Transportation, FAA, Washington D.C. January 1983

15. AGARD AR 159 "Fidelity of Simulation for Pilot Training".
AMP and FMP Advisory Report. December 1980

16. NASA Technical Paper 1540 "Application of Modified Profile Analysis to Function Testing of the Motion/No Motion Issue in an Aircraft Ground Handling Simulation".
R.V. Parrish, B.T. McKissick, G.G. Steinmetz December 1979

17. NASA CR 159331 "Advanced Flight Deck/Crew System Simulator Functional Requirements".
R.L. Wall, J.L. Tate, M.J. Moss. Lockheed, Georgia. December 1980

18. AGARD Report 432 "Simulator Assessment of Take-off and Landing".
A.G. Barnes. Specialists Meeting, Paris. January 1963

19. IFB 71 Proceedings of 1st European Simulation Congress. "IMPACS: Integrated Multi-Processor Aircraft Simulation System".
M.R. Southworth September 1983

20. NASA CR 145084 "Expansion of Flight Simulator Capability for Study and Solution of Aircraft Directional Control Problems on Runways - Phase I". March 1975

21. NASA CR 145044 "Expansion of Flight Simulator Capability for Study and Solution of Aircraft Directional control Problems on Runways". Phase II
August 1976

22. NASA CR-2970 "Expansion of Flight Simulator Capability for Study and Solution of Aircraft Directional Control Problems on Runways".
G.W. Kibbee. April 1978

23. NASA TM-81952 "Recent Progress Towards Predicting Aircraft Ground Handling Performance".
T.J. Yager and E.H. White. March 1981

24. SETP Conference, Lucerne, Switzerland "Thrust Reverser in JA 37 Viggen".
M. Moberg. 1972

25. Royal Aeronautical Society. Conference Proceedings - "Extending the Scope of Flight Simulation" London, 19 April 1978
"Experiences from Simulation of Aircraft Ground-Run Handling in the FOSIM Research Simulator"
Prof. S. Luthander April 1978

26. LUTAB-R-3046.2 "Simulation of the Landing Approach and Flare Manoeuvre".
A.G. Barnes, C-J Koivisto April 1981

27. LUTAB-R-3046.3 'Further Simulation of the Landing Approach and Flare Manoeuvre".
A.G. Barnes, C-J Koivisto, G. Holm, A. Hyden, R. Sundqvist
November 1982

28. Boeing report D6-49690-TN "Flight Test Correlation of the 727-200 Ground Handling Simulator"
J.J. Potter, S.K. Srinath July 1981

29. NASA TM 81250 "The Use of Total Simulator Training in Transitioning Air-Carrier Pilots - A Field Evaluation."
R.J. Randle Jnr., T.A. Tanner, J.A. Hamerman, T.H. Showalter
January 1981

30. NASA CR 166404 "An Analysis of Airline Landing Flare Data based on Flight and Training Simulator Measurements."
R.K. Heffley, T.M. Shulman, W.F. Clement August 1982

APPENDIX A

NOTATION

The terms in this Appendix are used in the equations of motion of Appendix B.

MATH SYMBOLS	UNITS	DESCRIPTION
A_{BRK}	metres^2	effective braking area
$BKPED_L$, $BKPED_R$	volts	normalized toe brake deflection, left and right
$BKPED_{L(BIAS)}$, $BKPED_{R(BIAS)}$	volts	biases on brake pedal inputs
$BKPED_{L(CMD)}$, $BKPED_{R(CMD)}$	volts	commanded brake pedal inputs
B^T_{jG}	-----	transformation matrix: j^{th} gear to A/C body
B^T_{jGV}	-----	transformation matrix: j^{th} gear velocity to A/C body
B^T_H	-----	transformation matrix: horizontal plane to A/C body
B^T_{LV}	-----	transformation matrix: local vertical to A/C body
bw	metres	wing span
$\bar{c}$	metres	wing mean aerodynamic chord
$C_{DAMP(j)}$	Newton/metre/second	strut linear damping coefficient
C_{ij}	unitless	coefficient of 3 x 3 matrix $[C_{11} - C_{33}]$
$C_{l\ TOTAL}$	unitless	total aero rolling moment coefficient in body axis
$C_{m\ TOTAL}$	unitless	total aero pitching moment coefficient in body axis
$C_{n_{TOTAL}}$	unitless	total aero yawing moment coefficient in body axis
$C_{X_{TOTAL}}$	unitless	total force coefficient in x-axis
$C_{Y_{TOTAL}}$	unitless	total force coefficient in y-axis
$C_{Z_{TOTAL}}$	unitless	total force coefficient in z-axis
C_{TM}, C_{TN}	Newton/metre/second	main and nose tire linear damping coefficients
CR_{jG}	metres	distance from runway centerline to a gear
CV_j	Newton/(metre/second)^2	strut velocity squared damping coefficient
CY_{RCT}, CY_{LCT}	seconds	Amount of time during anti-skid cycle right and left

MATH SYMBOLS	UNITS	DESCRIPTION
CY_{RCP}, CY_{LCP}	seconds	anti-skid cycle period, right and left
$C_{L_{TO(STATIC)}}$	seconds	static coefficient of lift, tail off
$C_{L'_{\alpha(H)}}$	unitless	elastic to rigid factor, for effect of stabilizer on lift
$C_{\ell_{TO(STATIC)}}$	unitless	static rolling moment, tail off
$C_{m_{TO(STATIC)}}$	unitless	static coefficient of pitch, tail off
$C_{n_{TO(STATIC)}}$	unitless	static yawing moment, tail off
$C_L[\alpha, \delta_F]$	unitless	contribution of angle of attack and flaps to static lift coefficient
$C_m[\alpha, \delta_F]$	unitless	contribution of angle of attack and flaps to static pitching moment coefficient
C_{L_H}	unitless	coefficient of lift for horizontal stabilizer
C_{m_H}	unitless	coefficient of pitching moment for horizontal stabilizer
C_{Y_V}	unitless	coefficient of side force on vertical tail
C_{L_α}	unitless	coefficient of lift due to angle of attack
$C_{L_{\alpha(V)}}$	unitless	coefficient of lift due to angle of attack on on vertical tail
$C_{L_{\alpha(H)}}$	unitless	coefficient of lift of horizontal stabilizer due to angle of attack
$C_{L_{\dot{\alpha}(H)}}$	unitless	coefficient of lift of horizontal stabilizer due to $\dot{\alpha}$
$C_{L_{\dot{\alpha}(TO)}}$	unitless	coefficient of lift due to angle of attack rate, tail off
$C_{m_{\dot{\alpha}(TO)}}$	unitless	coefficient of pitching moment due to angle of attack rate, tail off
$C_{L_{n(TO)}}$	unitless	coefficient of lift due to normal acceleration, tail off
$C_{m_{n(TO)}}$	unitless	coefficient of pitch due to normal acceleration, tail off
$C_{L_{n(H)}}$	unitless	coefficient of lift due to normal acceleration on the horizontal stabilizer
$C_{Y_{n_Y}}$	unitless	coefficient of side force due to lateral acceleration
$C_{L_{TO}}$	unitless	coefficient of lift with tail off
$C_{m_{TO}}$	unitless	coefficient of pitching moment with tail off
$C_{Y_{TO}}$	unitless	side force coefficient with tail off
$C_{L_{q(TO)}}$	unitless	coefficient of lift due to pitch rate with tail off
$C_{m_{q(TO)}}$	unitless	coefficient of pitching moment due to pitch rate with tail off
$C_{L_{q(H)}}$	unitless	coefficient of lift of horizontal stabilizer for pitch rate

MATH SYMBOLS	UNITS	DESCRIPTION
C_D	unitless	drag coefficient
C_T	unitless	coefficient of lift due to thrust
C_{X_S}	unitless	coefficient of drag, stability axis
C_{Z_S}	unitless	total lift coefficient, stability axis
$C_Y [\delta_r]$	unitless	total coefficient of side load due to rudder
$C_{Y_{\delta_r}}$	unitless	coefficient of side load due to rudder
$C_{Y'_{\delta_r}}$	unitless	elastic to rigid factor for effect of rudder on side load
$C_{L_{\delta_e}}$	unitless	coefficient of lift of horizontal stabilizer for δ_e
$C_{L'_{\delta_e}}$	unitless	rigid to elastic factor for effect of elevator on lift coefficient
$C_{\ell_{\delta_a}}$	unitless	coefficient of rolling moment due to aileron deflection
$C'_{\ell_{\delta_a}}$	unitless	rigid to elastic factor for effect of ailerons on rolling moment
$C_{n_{\delta_a}}$	unitless	coefficient of yawing moment due to aileron deflection
$C_{\ell_{\delta_{SP}}}$	unitless	coefficient of rolling moment due to spoiler deflection
$C_\ell [\alpha, \delta_{SP}, \delta_F]$	unitless	coefficient of rolling moment due to spoiler, flap deflection and angle of attack
$C_n [\alpha, \delta_{SP}, \delta_F]$	unitless	coefficient of yawing moment due to spoiler, flap deflection and angle of attack
$C_{\ell_{\beta(TO)}}$	unitless	coefficient of rolling moment due to sideslip angle, tail off
$C_{n_{\beta\,(TO)}}$	unitless	coefficient of yawing moment due to sideslip angle, tail off
$C_{Y_{\beta\,(TO)}}$	unitless	coefficient of side force due to sideslip angle, tail off
$C_{Y_{\dot{\beta}}}$	unitless	coefficient of side force due to sideslip angle rate
$C_{Y_{\beta(V)}}$	unitless	coefficient of side force due to sideslip angle on vertical tail
$C_{\ell_{\beta 1}}$, $C_{\ell_{\beta 2}}$	unitless	intercept points, function of angle of attack and flap angle
$C_{\ell_{P(TO)}}$	unitless	coefficient of rolling moment due to roll rate, tail off
$C_{n_{p(TO)}}$	unitless	coefficient of yawing moment due to roll rate, tail off
$C_{Y_{P(TO)}}$	unitless	coefficient of side force due to roll rate, tail off
$C_{Y_{P(V)}}$	unitless	coefficient of side force due to roll rate on vertical tail
C_{ℓ_p}	unitless	coefficient of rolling moment due to roll rate

MATH SYMBOLS	UNITS	DESCRIPTION
$C_{\ell_{\dot{p}}}$	unitless	coefficient of rolling moment due to rolling acceleration
$C_{Y_{\dot{p}(V)}}$	unitless	coefficient of side force due to roll acceleration on vertical tail
$C_{\ell_{r(TO)}}$	unitless	coefficient of rolling moment due to yaw rate, tail off
$C_{n_{r(TO)}}$	unitless	coefficient of yawing moment due to yaw rate with tail off
$C_{Y_{e(V)}}$	unitless	coefficient of side force due to yaw rate on vertical tail
$C_{Y_{\dot{r}}}$	unitless	coefficient of side force due to yaw acceleration
$C_{D_{i(GE)}}$	unitless	coefficient of induced drag due to ground effects
$C_{D_i}[\delta_F]$	unitless	coefficient of induced drag
$C_{D_p}[\delta_F]$	unitless	coefficient of parasitic drag
d_j	metres	current strut length of the j^{th} strut
d_{jS3}	metres	transform of Z component of j^{th} strut from gear velocity to gear axis system
$d_{V,cg}$	metres	vertical distance from c.g. to aerocenter of vertical stabilizer
d_{V,cg_r}	metres	vertical distance from c.g. to aerocenter of rudder surface
EPR_K	unitless	engine pressure ratios
E_{RWY}	metres	distance east, from the cg to the runway longitude line
f( )	-----	terminology symbolizing "a function of some variable"
FB_{CMD}	Newtons	commanded braking force
FB_{ON}	Newtons	braking force applied during the brake "on portion of the anti-skid cycle period"
$F_{DAMP(j)}$	Newtons	strut damping force
F_{GEAR}	Newtons	total force vector resulting from gear action
$F_{GW(j)}$	Newtons	"j^{th}" strut force
F_H	unitless	horizontal stabilizer bending factor
$F_{jA/C}$	Newtons	force vector acting on the j^{th} gear in the body axis system
F_{jB}	Newtons	braking force
F_{jE}	Newtons	normal force acting on the tire at the ground
$\bar{F}_{jG}$	Newtons	force vector in the gear axis system
$\bar{F}_{jGV}$	Newtons	force vector at the tire in the j^{th} gear velocity axis system
F_{jTD}	Newtons	tire damping force

MATH SYMBOLS	UNITS	DESCRIPTION
F_{jTS}	Newtons	tire spring force
$F_{SPRING(j)}$	Newtons	strut spring force
F_V	unitless	fuselage bending lateral plane
f $[X_{cg}]$	metres	normalized distance between c.g. and center of lift
g	9.81 metres/ second ^{2}	gravitational acceleration
GS_{ANGLE}	degrees	glide path angle
GS_{ERR}	volts	glide slope error
h_{cg}	metres	altitude of the aircraft measured at the cg
h_{DOWN}	metres	altitude
$\dot{h}_{DOWN}$	metres/second	rate of climb
h_{jBMP}	metres	height of the roughness bump at the wheel
h_{jCRN}	metres	height of the runway crown at the wheel
h_{jRWY}	metres	total height of the runway at the location of the j^{th} wheel
h_{jW}	metres	altitude of the j^{th} wheel hub
h_{RCL}	metres	height of the runway crown at the center line
H^T_{jg}	-----	transformation matrix: gear to horizontal
H^T_{LV}	-----	transformation matrix: local vertical to horizontal
IAS	knots	indicated airspeed
i°_H	degrees	horizontal stabilizer angle of incidence
IP_{jN}	unitless	integerized from of P_{jN}
Ixx, Iyy, Izz	kilogram-metres^2	body moments of inertia, x, y, and z axes
Ixz	kilogram-metres^2	cross product of moments of inertia in x and z axes
jG^T_H	-----	transformation matrix: horizontal to j^{th} gear
jG^T_{jGV}	-----	transformation matrix: j^{th} gear velocity to j^{th} gear
jGV^T_{jG}	-----	transformation matrix: j^{th} gear to j^{th} gear velocity
K_{GE}	unitless	ground effect factor, function of gear altitude (hwheel)
K_{GEAR}	unitless	factor which represents gear position (UP=0, DOWN=1)
k_{TM}	Newtons/metre	spring constant of left, right gear tire

MATH SYMBOLS	UNITS	DESCRIPTION
k_{TN}	Newtons/metre	spring constant of nose tire
L_A	metre-Newtons	aerodynamic rolling moment body axis
L_{ENG}	metre-Newtons	rolling moment due to the engines
$l_{H,cg}$	metres	distance from cg to horizontal stabilizer
$l_{H,\bar{c}/4}$	metres	intermediate distance used to determine $l_{V,cg}$
LOC_{ERR}	degrees	localizer error
l_{RGH}	metres	length of the section of roughness data
L_{TOTAL}	metre-Newtons	total aerodynamic rolling moment, body axis
Lu	metres	scale length used in the turbulence model
Lv	metres	scale length used in the turbulence model
Lw	metres	scale length used in the turbulence model
$l_{V,cg}$	metres	longitudinal distance from cg to vertical stabilizer
l_{V,cg_r}	metres	longitudinal distance from cg rudder surface
$l_{X,cg}$	metre-Newtons	longitudinal distance from cg at 25% MAC to actual cg (=0. for cg at 25% MAC)
m	kilograms	vehicle mass
M	-----	mach number
M_A	metre-Newtons	aerodynamic pitching moment body axis
M_{ENG}	metre-Newtons	pitching moment due to the engines
$\bar{M}_{GEAR}$	metre-Newtons	total moment acting at the A/C's cg as a result of gear action
$\bar{M}_{jA/C}$	metre-Newtons	moment about the cg due to forces on the j^{th} gear
M_{TOTAL}	metre-Newtons	total aerodynamic pitching moment, body axis
mu_j	kilograms	unsprung mass (i.e., combined mass of strut, wheel, and tire)
N_A	metre-Newtons	aeroydnamic yawing moment, body axis
N_{ENG}	metre-Newtons	yawing moment due to the engines
N_{RWY}	metres	distance north from the cg to the end of runway reference point
N_{TOTAL}	metre-Newtons	total aerodynamic yawing moment, body axis
n_X	g's	total longitudinal acceleration, body axis
n_Y	g's	total lateral acceleration, body axis
n_Z	g's	total normal (vertical) acceleration, body axis

MATH SYMBOLS	UNITS	DESCRIPTION
$ORF_{AREA(j)}$	$metres^2$	orifice area of j^{th} strut
P_B	radians/second	roll rate in body axis
$\dot{P}_B$	$radians/second^2$	roll acceleration in body axis
$P_{B(LAG)}$	degrees/second	lag in roll rate for yaw damper
P_{cg}	metres	distance along the runway from the EOR point to the cg.
P_{jN}	unitless	number of data sectors between j^{th} wheel location and end of runway
P_{jRGH}	metres	location of the j^{th} wheel within a roughness sector
P_{jRWY}	metres	Position of the j^{th} gear on the runway
P_{MG}	degrees	angle between A/C station line and main strut center line
P_{NG}	degrees	angle between A/C station line and nose strut centerline
P_{RES}	$Newtons/metres^2$	atmospheric pressure
P_S	degrees/second	roll rate, stability axis
$\bar{q}$	$Newtons/metres^2$	dynamic pressure
q_B	radians/second	pitch rate in body axis
$\dot{q}_B$	$radians/second^2$	pitch acceleration, body axis
r_B	radians/second	yaw rate in body axis
$\dot{r}_B$	$radians/second^2$	yaw acceleration, body axis
$r_{B(LAG)}$	degrees	lag in yaw rate for yaw damper
$r_{B(WASH)}$	degrees	yaw rate washout for yaw damper
r_S	radians/second	yaw rate, stability axis
$\bar{R}_j$	-----	radius vector from A/C cg to the j^{th} wheel hub
R_{jTD}	metres	deflected radius of the j^{th} tire
R_{LG}, R_{RG}	degrees	angle the left, right main strut makes with A/C buttline
RPM_k	/second	engine revolutions per minute
R_{TIM}, R_{TIN}	metres	inflated radius of main, nose tire
RWY_s	metres	runway slope
RWY_w	metres	runway width
s	-----	Laplace transform
SF	-----	scale factor

MATH SYMBOLS	UNITS	DESCRIPTION
$SK_{ANG(j)}$	degrees	skid angles of j^{th} wheel
SSK_j	-----	sign control term
S_w	$metres^2$	wing area
t	seconds	time
T	Newtons	total thrust
T_k	Newtons	thrust for each engine
T_K°	degrees	temperature, Kelvin scale
u_A	metres/second	resultant velocity, body x-axis
$\dot{u}_A$	$metres/second^2$	resultant acceleration, body x-axis
u_B	metres/second	aircraft velocity, body axis
$\dot{u}_B$	$metres/second^2$	aircraft translational acceleration, body x-axis
$\dot{u}_{B(g)}$	$metres/second^2$	gravitational component, body x-axis
u_G	metres/second	gust component, body x-axis
$\dot{u}_G$	$metres/second^2$	gust acceleration in body x-axis
$u_{G(I)}$	metres/second	gust component along x-earth axis
u_W	metres/second	wind component along body x-axis
$u_{W(I)}$	metres/second	wind component along x-earth axis
v_A	metres/second	resultant velocity, body y-axis
$\dot{v}_A$	$metres/second^2$	resultant acceleration, body y-axis
$\dot{v}_{A(T)}$	$metres/second^2$	rate of change of total flight velocity
v_B	metres/second	aircraft velocity, body y-axis
$\dot{v}_B$	$metres/second^2$	translational acceleration along body y-axis
$\dot{v}_{B(g)}$	$metres/second^2$	gravitational component, body y-axis
v_G	metres/second	gust component in body y-axis
$\dot{v}_G$	$metres/second^2$	gust acceleration in y-axis
$v_{G(I)}$	metres/second	gust component, y-earth axis
$\bar{V}_G$	metres/second	A/C velocity vector in local vertical system
V_{GROUND}	knots	ground speed
V_I	metres/second	true velocity
V_{jH}	metres/second	wheel velocity
$\bar{V}_{jR}$	metres/second	velocity vector at wheel due to A/C rotations, body system

MATH SYMBOLS	UNITS	DESCRIPTION
V_{jRE}	metres/second	velocity vector at wheel due to A/C rotations, local vertical system
$V_{j(TOTAL)}$	metres/second	total velocity at the gear
$\bar{V}_{jTW}$	metres/second	total velocity vector at the wheel, local vertical system
$\bar{V}_{jW}$	metres/second	total velocity vector at the wheel A/C body system
V_{SOUND}	metres/second	speed of sound
V_{TOTAL}	metres/second	total flight path velocity
v_W	metres/second	wind component along body y-axis
$v_{W(I)}$	metres/second	wind component along y-earth axis
w_A	metres/second	resultant velocity, body z-axis
$\dot{w}_A$	metres/second^2	resultant acceleration, body z-axis
w_B	metres/second	normal velocity, body z-axis
$\dot{w}_B$	metres/second^2	translational acceleration along body z-axis
$\dot{w}_{B(g)}$	metres/second^2	gravitational component, body z-axis
w_G	metres/second	gust component, body z-axis
$\dot{w}_G$	metres/second^2	gust acceleration, body z-axis
$w_{G(I)}$	metres/second	gust component, earth z-axis (down)
$WIND_{DIR}$	radians	wind direction
$WIND_{MG}$	metres/second	wind magnitude
WT	Newtons	aircraft weight
$WT_{STRUT(j)}$	Newtons	unsprung weight of the j^{th} strut
w_W	metres/second	wind component along body z-axis
X_A	Newtons	aerodynamic force in body x-axis
X_{cg}	percent	center of gravity
X_{ENG}	Newtons	thrust in body x-axis due to engines
X_{NORTH}	metres	distance north, earth axis system
$\dot{X}_{NORTH}$	metres/second	earth axis velocity, North (x-axis)
$X_{p,cg}$	metres	x distance from cg to the pilot's eye
Xs_k	degrees	throttle input
$\dot{X}_{s_k}$	degrees/second	rate of change of throttle input
X_{s_k} (past)	degrees	past value of throttle input

MATH SYMBOLS	UNITS	DESCRIPTION
Y_A	Newtons	aerodynamic force in body y-axis
$Y_{DAMP(1)}$, $Y_{DAMP(2)}$	degree	yaw damping intermediate term
$\dot{Y}_{DAMP(1)}$ $\dot{Y}_{DAMP(2)}$	degree/second	yaw damping intermediate integration
Y_E	metres	distance between engines
Y_{EAST}	metres	distance east, earth y-axis
$\dot{Y}_{EAST}$	metres/second	earth axis velocity, east (y-axis)
Y_{ENG}	Newtons	aero force in body y-axis due to engines
$Y_{p,cg}$	metres	y distance from cg to pilot's eye
Z_A	Newtons	aerodynamic force in body z-axis
$Z_{DAMP\ (1)}$	degrees	yaw damping intermediate term
$\dot{Z}_{DAMP(1)}$	degrees/second	yaw damping intermediate integration
Z_E	metres	height of thrust line above c.g.
Z_{ENG}	Newtons	aerodynamic force due to the engines
$Z_{p,cg}$	metres	z distance from cg to pilot's eye
α	radians	angle of attack (angle between flight path velocity and x-body axis)
α°	degrees	angle of attack in degrees
α_H , (α_H°)	radians	horizontal stabilizer angle of attack, (in degrees)
$\dot{\alpha}$	radians/second	rate of change of angle of attack
β	radians	sideslip angle
β°	degrees	sideslip angle in degrees
$\dot{\beta}$	radians/second	rate of change of slideslip angle
$\Delta C_D\ [\delta_{SB}]$	unitless	increment of drag coefficient due to speed brake
$\Delta C_{D\ (GEAR)}$	unitless	contribution of gear to drag coefficient
$\Delta C_{L(GEAR)}$	unitless	contribution of landing gear to static lift
$\Delta C_{L(GE)}[\alpha, \delta_F]$	unitless	contribution of ground effects to static lift
$\Delta C_{L(TO)}$	unitless	increment in lift to account for structural elasticity
$\Delta C_L[\delta_{SB}]$	unitless	increment in lift coefficient due to speed brake
$\Delta C_{\ell_{\beta\ (CLTO=0)}}$	unitless	increment in C_{ℓ_β} due to lift coefficient, tail off

MATH SYMBOLS	UNITS	DESCRIPTION
$\Delta C_{\ell_{\beta(TO=0)_{TO}}}$	unitless	C_{ℓ_β} increment, tail off
$\left[\frac{\partial C_{\ell_A}}{\partial C_L}\right]_{TO}$	unitless	derivative of C_{ℓ_β} with respect to lift coefficient, tail off
$\Delta C_{m_{GEAR}}$	unitless	contribution of gear to static pitching moment coefficient
$\Delta C_{M_{O(TO)}}$	unitless	increment in pitching moment coefficient, tail off
$\Delta C_{m_{TO}}$	unitless	increment in pitch coefficient, tail off
$\Delta C_{m_{GE}}[\alpha, \delta_F]$	unitless	increment in pitching moment due to ground effects
$\Delta C_m[\delta_{SB}]$	unitless	increment in pitching moment coefficient due to speed brake
ΔCR_{cg}	metres	lateral distance from runway centerline to aircraft cg
ΔCR_{jG}	metres	lateral distance from aircraft cg to j^{th} gear
ΔP_{jG}	metres	distance along runway from cg to j^{th} gear
$\Delta\epsilon_{GE}[\alpha, \delta_F]$	unitless	downwash increment due to ground effects
$\Delta\epsilon[\delta_{SB}]$	unitless	increment in horizontal stabilizer downwash angle due to speed brake
$\Delta\psi$	degrees	difference between euler yaw angle ψ and runway heading
δ_a	degrees	aileron deflection
δ_{COL}	metres	column deflection
$\delta_{COL(O)}$	metres	initial column position
$\delta_{COL\ (TRIM)}$	metres	column trim position
δ_e	degrees	elevator deflection
δ_F	degrees	flap angle
δ_{jT}	metres	j^{th} tire deflection
$\dot{\delta}_{jT}$	metres/second	rate of compression of j^{th} tire
δ_{PEDAL}	metres	rudder pedal deflection
δ_r	degrees	rudder deflection
δ_{SB}	degrees	speed brake deflection
$\delta_{STRUT(j)}$	metres	deflection of j^{th} strut
$\dot{\delta}_{STRUT(j)}$	metres/second	rate of compression of j^{th} strut
$\ddot{\delta}_{STRUT(j)}$	metres/second^2	acceleration of j^{th} gear
δ_{THk}	degrees	throttle input

MATH SYMBOLS	UNITS	DESCRIPTION
$\delta_{THk(BIAS)}$	degrees	throttle bias
$\delta_{THk(CMD)}$	degrees	commanded throttle
δ_{SP}	degrees	spoiler deflection
$\dot{\delta}_{SB}$	degrees/second	speed brake rate of deflection
$\dot{\delta}_{SB(CMD)}$	degrees/second	commanded speed brake rate of deflection
δ_{w}	degrees	control wheel deflection
ε_{YD}	metres	yaw damper deflection
ε°	degrees	horizontal stabilizer downwash angle
$\varepsilon_{1}[\alpha, \delta_{F}]$	degrees	contribution to due to angle of attack and flaps
$\frac{\partial C_L}{\partial C_T}[\delta_F]$	unitless	change in lift with respect to the change in thrust due to flaps
$\left[\frac{\partial C_m}{\partial C_L}\right]_{To}$	unitless	derivative of pitching moment with respect to change in lift, tail off
$\left[\frac{\partial C_{\ell\beta}}{\partial C_n}\right]_{To}$	unitless	derivative of $C_{\ell\beta}$ with respect to the change in yawing moment, tail off
γ	radians	flight path angle
γ°	degrees	flight path angle in degrees
μ_{D_j}	unitless	braking coefficient of friction of j^{th} gear with anti-skid operating
μ_{S_j}	unitless	side force coefficient of friction j^{th} gear
ϕ	radians	aircraft roll attitude angle
$\dot{\phi}$	radians/second	roll rate (body axes)
ϕ°	degrees	roll angle in degrees
ψ	radians	aircraft yaw attitude angle
$\dot{\psi}$	radians/second	yaw rate (body axes)
ψ°	degrees	yaw angle in degrees
ψ_{Gj}	radians	angle of j^{th} gear used when determining j^{th} gear spring force
ψ_{jW}	degrees	angle between the velocity vector at the j^{th} wheel and the long axis X_H in the horizontal axis system
ψ_{RWY}	degrees	heading of the runway from the north
π	3.14159	circumference/diameter of a circle
ρ	kilogram/metres^3	air density
σ_u	knots	RMS gust intensity

MATH SYMBOLS	UNITS	DESCRIPTION
σ_v	knots	RMS gust intensity
σ_w	knots	RMS gust intensity
σ_N	degrees	nose wheel steering angle
τ	seconds	time constant
θ	radians	pitch angle
$\dot{\theta}$	radians/second	pitch angle rate
θ°	degrees	pitch angle degrees
$\bar{\omega}$	radians/second	aircraft body rotation vector
ξ_T	degrees	angle thrust makes with the fuselage

ABBREVIATIONS

A/C	-----	aircraft
B	-----	subscript for A/C body axis
F	Newtons	general force
i	-----	subscript index to indicate terms that differ between the nose and main gear system i=m,n
j	-----	subscript to indicate to which particular gear a term applies, j = L for left gear = R for right gear = N for nose gear
ij	_____	subscripts ranging from 1-3 indicating elements of a matrix
k	_____	subscript ranging from 1-2 indicating engine No. 1 or engine No. 2

APPENDIX B

EQUATIONS OF MOTION

The equations of motion in this Appendix were used for the research work described in section 5.1.2. Although the formulation may not be appropriate to every application (see the discussion in para. 3.1), they illustrate:

(a) the structural form of the equations,

(b) the breakdown into individual blocks,

(c) the axis system which must be respected,

(d) the magnitude of the computing task,

(e) the form of the information needed to complete the model.

AXIS SYSTEM DEFINITIONS

All axis systems used are made of three orthogonal axes that follow the right hand rotation rules.

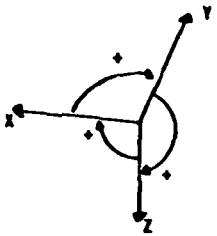

Right Hand Rotation

LOCAL VERTICAL AXIS SYSTEM

The Local Vertical (LV) axis system is defined by locating an axis down along the gravity vector toward the center of the Earth. The other two axes are located in a plane normal to the down axis. These two axes are oriented such that one points North and the other East as shown below. Hence, this system is sometimes referred to as a North, East, Down (N.E.D.) system.

LOCAL VERICAL AXIS

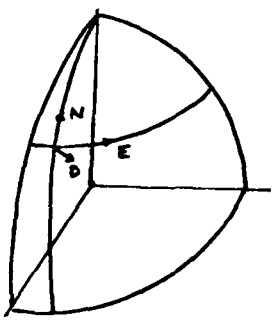

Earth Axis

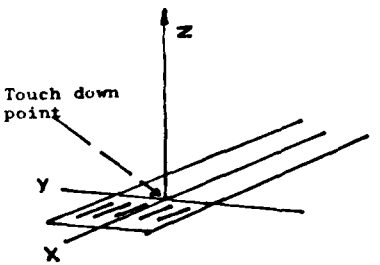

HORIZONTAL AXIS SYSTEM

This axis system also has one axis located down along the gravity vector toward the center of the Earth. The other two axes are orthogonal and lie in the horizontal plane; however, one is located along the projection of the aircraft's longitudinal axis on the horizontal plane and the other in the direction of the aircraft's right wing.

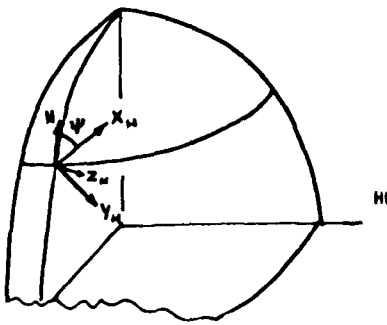

HORIZONTAL AXIS SYSTEM

The angle between the North axis and the X axis of this system is the Euler angle ψ .

AIRCRAFT BODY AXIS SYSTEM

This system is defined with the X-axis along the fuselage center line, positive forward. The Y-axis lies in the center plane of the aircraft, positive in the direction of the right wing and intersects the X-axis at the center of gravity of the aircraft. The Z-axis is then normal to the X-Y plane and positive through the bottom of the fuselage.

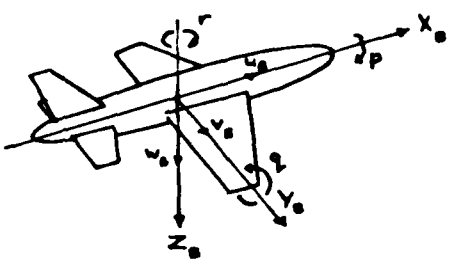

GEAR VELOCITY AXIS SYSTEMS

The GEAR velocity axis systems are defined at each wheel. As shown below, the X-axis is defined to lie along the component of the local velocity at the wheel in the horizontal plane. The Y-axis is in the horizontal plane and positive to the right of the aircraft. The Z-axis is down, normal to the horizontal plane.

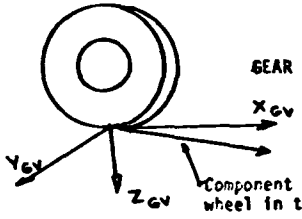

GEAR VELOCITY AXIS SYSTEM

Component of the velocity at the wheel in the horizontal plane

LANDING GEAR AXIS SYSTEMS

The Z-axes of the Landing Gear axis systems are defined as positive down along the gear struts. The X and Y axes are then orthogonal to the struts with the X axis positive forward and the Y axis positive toward the right side of the aircraft.

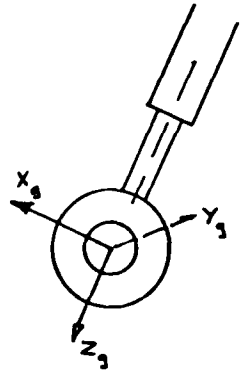

LANDING GEAR AXIS SYSTEM

Aircraft Geometry

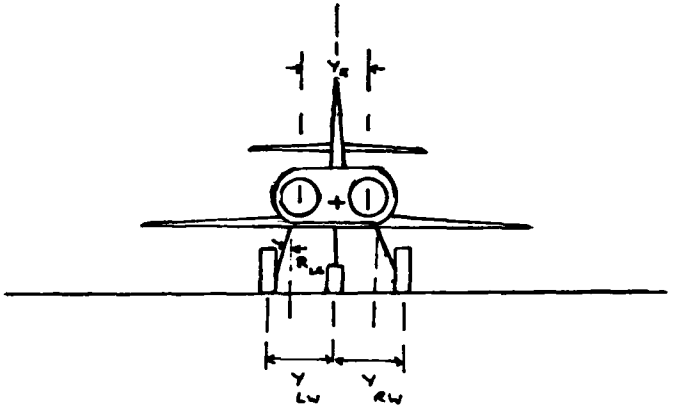

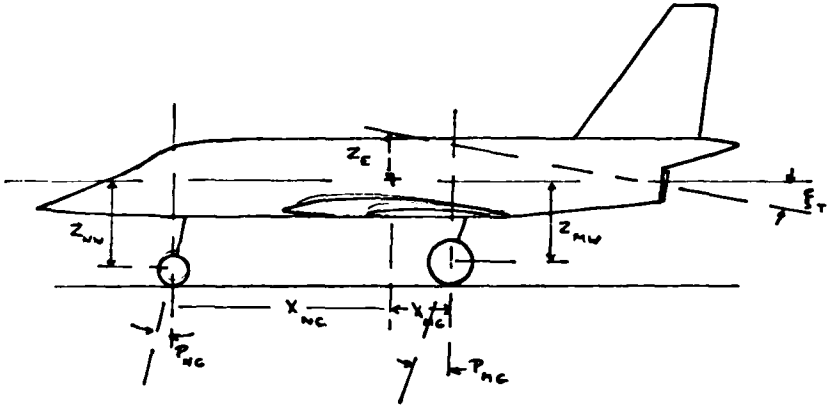

AERODYNAMIC FORCES IN BODY AXIS

$$X_A = \bar{q}\, S_w\, C_{X_{TOTAL}}$$

$$Y_A = \bar{q}\, S_w\, C_{Y_{TOTAL}}$$

$$Z_A = \bar{q}\, S_w\, C_{Z_{TOTAL}}$$

AERODYNAMIC MOMENTS IN BODY AXIS

$$L_A = \bar{q}\, S_w\, bw\, C_{\ell_{TOTAL}}$$

$$M_A = \bar{q}\, S_w\, \bar{c}\, C_{m_{TOTAL}}$$

$$N_A = \bar{q}\, S_w\, bw\, C_{n_{TOTAL}}$$

AERO VELOCITIES, ANGLES, ACCELERATIONS

$$\alpha = \tan^{-1}\left(w_A / v_A\right)$$

$$\beta = \sin^{-1}\left(v_A / V_{TOTAL}\right)$$

$$V_{TOTAL} = \sqrt{u_A^2 + v_A^2 + w_A^2}$$

$$V_I = \sqrt{u_B^2 + v_B^2 + w_B^2}$$

$$u_A = u_B - u_G - u_W$$

$$v_A = v_B - v_G - v_W$$

$$w_A = w_B - w_G - w_W$$

$$\dot{u}_A = \dot{u}_B - \dot{u}_G - \left(q_B w_G - r_B v_G\right)$$

$$\dot{v}_A = \dot{v}_B - \dot{v}_G - \left(r_B u_G - p_B w_G\right)$$

$$\dot{w}_A = \dot{w}_B - \dot{w}_G - \left(p_B v_G - q_B u_G\right)$$

$$\dot{\alpha} = u_A \dot{w}_A - w_A \dot{u}_A \Big/ \left(V_{TOTAL}\right)^2$$

$$\dot{V}_{A(T)} = \left(u_A \dot{u}_A + v_A \dot{v}_A + w_A \dot{w}_A\right) \Big/ V_{TOTAL}$$

$$\dot{\beta} = \left(V_{TOTAL}\, \dot{v}_A - v_A\, \dot{V}_{A(T)}\right) \Big/ \left(V_{TOTAL}\right)^2 \cos(\beta)$$

ATMOSPHERIC VARIABLES

$$\bar{q} = \tfrac{1}{2} \rho\, V_{TOTAL}^2 \qquad \rho = f\left(h_{DOWN}\right) \qquad T_K^\circ = f\left(h_{DOWN}\right)$$

$$M = V_{TOTAL} / V_{SOUND} \qquad P_{RES} = f\left(h_{DOWN}\right) \qquad V_{SOUND} = f\left(h_{DOWN}\right)$$

$$IAS = \left(V_{TOTAL} \sqrt{\rho \,/\, 1.2256}\right) 1.9427$$

DIRECTION COSINE MATRIX

$$C_{11} = \cos\psi \cos\theta \qquad C_{31} = \sin\phi \sin\psi + \cos\phi \sin\theta \cos\psi$$

$$C_{12} = \sin\psi \cos\theta \qquad C_{32} = -\sin\phi \cos\psi + \cos\phi \sin\theta \sin\psi$$

$$C_{13} = -\sin\theta \qquad C_{33} = \cos\theta \cos\phi$$

$$C_{21} = -\cos\phi \sin\psi + \sin\phi \sin\theta \cos\psi$$

$$C_{22} = \cos\phi \cos\psi + \sin\phi \sin\theta \sin\psi$$

$$C_{23} = \sin\phi \cos\theta$$

BODY AXIS ACCELERATIONS

$$n_X = \left(\dot{u}_B - u_{B(g)} + w_B q_B - v_B r_B\right) / g$$

$$n_Y = \left(\dot{v}_B - v_{B(g)} + u_B r_B - w_B p_B\right) / g$$

$$n_Z = -\left(\dot{w}_B - w_{B(g)} + v_B p_B - u_B q_B\right) / g$$

EARTH AXIS VELOCITIES, AUXILARY ANGLES

$$\dot{X}_{NORTH} = C_{11}\, u_B + C_{21}\, v_B + C_{31}\, w_B$$

$$\dot{Y}_{EAST} = C_{12}\, u_B + C_{22}\, v_B + C_{32}\, w_B$$

$$\dot{h}_{DOWN} = -C_{13}\, u_B - C_{23}\, v_B - C_{33}\, w_B$$

$$V_{GROUND} = \left(\sqrt{\dot{X}^2_{NORTH} + \dot{Y}^2_{EAST}} \right)$$

$$GS_{ERR} = GS_{ANGLE} - \tan^{-1}\left(h_{DOWN} / \left| X_{NORTH} - 1000. \right| \right) \quad (57.3)$$

$$= 0. \quad \text{if } X_{NORTH} > 1000.$$

$$LOC_{ERR} = -\tan^{-1}\left(Y_{EAST} / \left| X_{NORTH} \right| \right) \quad (57.3)$$

$$\gamma = \sin^{-1}\left(\dot{h}_{DOWN} / V_I \right)$$

ATTITUDE RATE EQUATIONS

$$\dot{\psi} = \left(r_B \cos\phi + q_B \sin\phi \right) / \cos\theta$$

$$\dot{\theta} = q_B \cos\phi - r_B \sin\phi$$

$$\dot{\phi} = p_B + \dot{\psi} \sin\theta$$

STABILITY RATES

$$p_S = p_B \cos\alpha + r_B \sin\alpha$$

$$r_S = -p_B \sin\alpha + r_B \cos\alpha$$

GRAVITATIONAL ACCELERATIONS IN BODY AXIS

$$u_{B(g)} = g\, C_{13}$$

$$v_{B(g)} = g\, C_{23}$$

$$w_{B(g)} = g\, C_{33}$$

ROTATIONAL ACCELERATIONS IN BODY AXIS

$$L_{TOTAL} = L_A + L_{ENG} + M_{GEAR(1)}$$

$$M_{TOTAL} = M_A + M_{ENG} + M_{GEAR(2)}$$

$$N_{TOTAL} = N_A + N_{ENG} + M_{GEAR(3)}$$

$$\dot{p}_B = 1./Ix\ (Ix\ Iz/(Ix\ Iz - Ixz^2)) \left(L_{TOTAL} + (Ixz/Iz)\, N_{TOTAL} + q_B\, r_B\, (Iy - Iz - Ixz^2/Iz) \right) + Ixz/Iz\ p_B\, q_B\, (Ix + Iz - Iy))$$

$$\dot{q}_B = 1./Iy \left(p_B\, r_B\, (Iz - Ix) + Ixz \left(r_B^2 - p_B^2 \right) + M_{TOTAL} \right)$$

$$\dot{r}_B = 1./Iz \left(p_B\, q_B\, (Ix - Iy) + \left(\dot{p}_B - q_B\, r_B \right) Ixz + N_{TOTAL} \right)$$

TRANSLATIONAL ACCELERATIONS IN BODY AXIS

$$\dot{u}_B = u_{B(g)} + v_B\, r_B - w_B\, q_B + \left(\frac{X_A + X_{ENG} + F_{GEAR(1)}}{m} \right)$$

$$\dot{v}_B = v_{B(g)} + w_B\, p_B - u_B\, r_B + \left(\frac{Y_A + Y_{ENG} + F_{GEAR(2)}}{m} \right)$$

$$\dot{w}_B = w_{B(g)} + u_B\, q_B - v_B\, p_B + \left(\frac{Z_A + Z_{ENG} + F_{GEAR(3)}}{m} \right)$$

GUST MODEL

Dryden Spectra

$$\sigma u,\ \sigma v,\ \sigma w = f\left(h_{DOWN}\right)$$

$$\Phi_{G(I)}(s) = \sigma u \sqrt{Lu/\ 30.\pi}\ \frac{1}{1 + (Lu/\ 30.)\ s}$$

$$\Phi_{G(I)}(s) = \sigma v \sqrt{Lv/\ 60.\pi}\ \frac{1 + \sqrt{3}\ (Lv/\ 30.)\ s}{(1 + (Lv/\ 30.)\ s)^2}$$

$$\Phi_{G(I)}(s) = \sigma w \sqrt{Lw/\ 60.\pi}\ \frac{1 + \sqrt{3}\ (Lw/\ 30.)\ s}{(1 + (Lw/\ 30.)\ s)^2}$$

Gust Components in Body Axis

$$u_G = C_{11}\ u_{G(I)} + C_{12}\ v_{G(I)} + C_{13}\ w_{G(I)}$$

$$v_G = C_{12}\ u_{G(I)} + C_{22}\ v_{G(I)} + C_{23}\ w_{G(I)}$$

$$w_G = C_{13}\ u_{G(I)} + C_{23}\ v_{G(I)} + C_{33}\ w_{G(I)}$$

Gust Acceleration in Body Axis

$$\dot{u}_G = C_{11}\ \dot{u}_{G(I)} + C_{12}\ \dot{v}_{G(I)} + C_{13}\ \dot{w}_{G(I)}$$

$$\dot{v}_G = C_{21}\ \dot{u}_{G(I)} + C_{22}\ \dot{v}_{G(I)} + C_{23}\ \dot{w}_{G(I)}$$

$$\dot{w}_G = C_{31}\ \dot{u}_{G(I)} + C_{32}\ \dot{v}_{G(I)} + C_{33}\ \dot{w}_{G(I)}$$

WINDS

$$u_{W(I)} = \left(WIND_{MG}\right) \cos\left(WIND_{DIR}\right)$$

$$v_{W(I)} = \left(WIND_{MG}\right) \sin\left(WIND_{DIR}\right)$$

$$u_W = C_{11}\ u_{W(I)} + C_{12}\ v_{W(I)}$$

$$v_W = C_{21}\ u_{W(I)} + C_{22}\ v_{W(I)}$$

$$w_W = C_{31}\ u_{W(I)} + C_{32}\ v_{W(I)}$$

ENGINE MODEL

$$EPR_k = f\left(Xs_k\right) \qquad k = 1,\ 2$$

$$T_k = f\left(EPR_k,\ M\right)$$

$$T = T_1 + T_2$$

Engine Forces

$$X_{ENG} = T \cos\left(\varepsilon_T\right)$$

$$Y_{ENG} = 0.$$

$$Z_{ENG} = T \sin\left(\varepsilon_T\right)$$

Engine Moments

$$L_{ENG} = 0.$$

$$M_{ENG} = \left(T_1 + T_2\right) Z_\varepsilon$$

$$N_{ENG} = \left(T_1 - T_2\right) Y_\varepsilon$$

LONGITUDINAL AERO FORCE COEFFICIENTS

Lift Coefficient

$$C_T = T/\bar{q}\, S_w$$

$$K_{GE} = f\left(h_{wheel}\right)$$

$$C_{L_{TO(STATIC)}} = C_L\left(\alpha,\ \delta_F\right) + \Delta C_{L_{GE}}\left(\alpha,\ \delta_F\right) K_{GE} + \Delta C_{L_{GEAR}} K_{GEAR}$$

$$\frac{\partial C_L}{\partial C_T}\left(\delta_F\right) = C_{L_{TO(STATIC)}} C_{L_\alpha} + C_{L_{n(TO)}} n_Z$$

$$C_{L_{TO}} = C_{L_{TO(STATIC)}} + \Delta C_{L_{TO}} + \left[C_{L_{q(TO)}} q_B + C_{L_{\dot{\alpha}(TO)}} \dot{\alpha}\right] (57.3) \frac{\bar{c}}{2V_{TOTAL}} + \frac{\partial C_L}{\partial C_T}\left(\delta_F\right) C_T$$

Horizontal Stabilizer Component Of Total Lift

$$F_H = 1. - .00087\, \bar{q}$$

$$\epsilon^\circ = \epsilon_1\left(\alpha,\ \delta_F\right) + \Delta\epsilon_{GE}\left(\alpha,\ \delta_F\right) K_{GE} + \Delta\epsilon\left(\delta_{SB}\right)$$

$$\alpha_H^\circ = \alpha^\circ - \epsilon^\circ + i_H^\circ$$

$$C_{L_H} = F_H \left[\alpha_H C_{L'_{\alpha(H)}} C_{L_{\alpha(H)}} + C_{L_{n(H)}} n_Z + C_{L'_{\delta_e}} C_{L_{\delta_e}} \delta_e + C_{L_{\alpha(H)}}\left[C_{L_{q(H)}} q_B + C_{L_{\dot{\alpha}(H)}} \dot{\alpha}_H (57.3) \frac{\bar{c}}{2V_{TOTAL}}\right]\right]$$

Total Lift

$$C_{Z_S} = -\left(\left[C_{L_{TO}} + C_{L_H}\right] - \Delta C_L\left(\delta_{SB}\right)\right)$$

Pitching Moment Coefficient

$$K_{GE} = f\left(h_{wheel}\right)$$

$$C_{m_{TO(STATIC)}} = C_m\left(\alpha,\ \delta_F\right) + \Delta C_{m_{GE}}\left(\alpha,\ \delta_F\right) K_{GE} + \Delta C_{m_{GEAR}} K_{GEAR}$$

$$\Delta C_{m_{TO}} = \Delta C_{m_{O(TO)}} + \left[\frac{\partial C_m}{\partial C_L}\right]_{TO} C_{L_{TO}} - C_{m_{n(TO)}} n_Z$$

$$C_{m_{TO}} = C_{m_{TO(STATIC)}} + \Delta C_{m_{TO}} + C_{L_{TO}} f\left(X_{cg}\right) + \left[C_{m_{q(TO)}} q_B + C_{m_{\dot{\alpha}(TO)}} \dot{\alpha}\right] (57.3) \frac{\bar{c}}{2V_{TOTAL}}$$

Horizontal Stabilizer Component of Pitching Moment

$$C_{m_H} = -C_{L_H} l_{H,cg}$$

Total Pitching Moment

$$C_{m_{TOTAL}} = C_{m_{TO}} + C_{m_H} + \Delta C_m\left(\delta_{SB}\right)$$

Drag Coefficient

$$C_D = C_{D_P\left(\delta_F\right)}\left(\delta_F\right) + C_{D_{i(GE)}}\left(C_{Z_S}\right)^2 C_{D_1}\left(\delta_F\right) + \Delta C_{D(GEAR)} K_{GEAR} + \Delta C_D\left(\delta_{SB}\right)$$

Total Drag

$$C_{X_S} = -C_D$$

LATERAL-DIRECTIONAL AERO COEFFICIENTS

Rolling Moment Coefficient

$$C_{\ell_{\beta(TO)}} = C_{\ell_{\beta 1}}(\delta_F) + \Delta C_{\ell_{\beta(CLTO=0)}} + \left[C_{\ell_{\beta 2}}(\delta_F) - \left[\Delta\frac{\partial C_{\ell_\beta}}{\partial C_L}\right]_{TO}\right] C_{L_{TO}} + \left[\frac{\partial C_{\ell_\beta}}{\partial C_n}\right]_{TO} n_Z$$

Total Rolling Moment

$$C_{\ell_{TO(STATIC)}} = C_{\ell_{\beta(TO)}}\beta + C_{\ell_{\dot{p}}}\dot{p}_B\,(57.3) + C_{\ell_{p(TO)}} C_{\ell_p} p_S + C_{\ell_{r(TO)}} r_S \frac{bw}{2V_{TOTAL}}(57.3) + C_{\ell_{\delta_a}} C_{\ell'_{\delta_a}}\delta_a + C_{\ell_{\delta_{SP}}} C_\ell(\alpha, \delta_{SP}, \delta_F)$$

Yawing Moment

$$C_{n_{TO(STATIC)}} = C_{n_{\beta(TO)}}\beta^\circ + C_{n_{\delta_a}}\delta_a + C_n(\alpha, \delta_{SP}, \delta_F) + \left[C_{n_{p(TO)}} p_S + C_{n_{r(TO)}}\right]\frac{bw}{2V_{TOTAL}}(57.3)$$

Aero Moments to Body Axis

$$C_{\ell_{TOTAL}} = C_{\ell_{TO(STATIC)}}\cos\alpha - C_{n_{TO(STATIC)}}\sin\alpha + d_{V,cg} C_{Y_V} + d_{V,cg_r} C_Y(\delta_r)$$

$$C_{n_{TOTAL}} = C_{n_{TO(STATIC)}}\cos\alpha + C_{\ell_{TO(STATIC)}}\sin\alpha - l_{V,cg} C_{Y_V} - l_{V,cg} C_Y(\delta_r) - l_{X,cg} C_{Y_{TO}}$$

Side Force Coefficient

$$C_{Y_{TO}} = C_{Y_{\beta(TO)}}\beta^\circ + C_{Y_{p(TO)}} p_S \frac{bw}{2V_{TOTAL}}\,57.3$$

Side Force Due to Vertical Tail Without Rudder

$$C_{Y_V} = F_V\left[C_{L_{\alpha(V)}} C_{Y_{\beta(V)}}\beta^\circ + C_{Y_{\dot{r}}}\dot{r}_B\,(57.3) + C_{Y_{n_Y}} n_Y + C_{L_{\alpha(V)}}\left[C_{Y_{\dot{\beta}}}\dot{\beta} + C_{Y_p} p_B + C_{Y_{r(V)}} r_B + \frac{C_{Y_{\dot{p}(V)}}}{V_{TOTAL}}\dot{p}_B\right]\frac{bw}{2V_{TOTAL}}\,57.3\right]$$

Side Force Due to Rudder

$$C_Y(\delta_r) = F_V C_{Y_{\delta_r}} C_{Y_{\delta_r}}\delta_r$$

Total Side Force in Body Axis

$$C_{Y_{TOTAL}} = C_{Y_{TO}} + C_{Y_V} + C_Y(\delta_r)$$

Stability Coefficient to Body Axis

$$C_{X_{TOTAL}} = C_{X_S}\cos\alpha - C_{Z_S}\sin\alpha$$

$$C_{Z_{TOTAL}} = C_{X_S}\sin\alpha + C_{Z_S}\cos\alpha$$

TRANSFORMATION MATRICES

Local Vertical to Horizontal

$$H^{T}_{LV} = \begin{bmatrix} \cos\Psi & \sin\Psi & 0 \\ -\sin\Psi & \cos\Psi & 0 \\ 0 & 0 & 1 \end{bmatrix}$$

Horizontal to Aircraft Body

$$B^{T}_{H} = \begin{bmatrix} \cos\theta & 0 & -\sin\theta \\ \sin\phi\sin\theta & \cos\phi & \sin\phi\cos\theta \\ \cos\phi\sin\theta & -\sin\phi & \cos\phi\cos\theta \end{bmatrix}$$

Local Vertical to Aircraft Body

$$B^{T}_{LV} = \begin{bmatrix} \cos\theta\cos\Psi & \cos\theta\sin\Psi & -\sin\theta \\ (\sin\phi\sin\theta\cos\Psi - \cos\phi\sin\Psi) & (\sin\phi\sin\theta\sin\Psi + \cos\phi\cos\Psi) & \sin\phi\cos\theta \\ (\cos\phi\sin\theta\cos\Psi + \sin\phi\sin\Psi) & (\cos\phi\sin\theta\sin\Psi - \sin\phi\cos\Psi) & \cos\phi\cos\theta \end{bmatrix}$$

Horizontal to Gear

$${}_{jG}T_{H} = \left[B^{T}_{jG}\right]^{T}\left[B^{T}_{H}\right]$$

Gear Velocity to Gear

$${}_{jG}T_{jGV} = \left[{}_{jG}T_{H}\right]^{T}\left[H^{T}_{jGV}\right]$$

Gear Velocity to Aircraft Body

$$B^{T}_{jGV} = \left[B^{T}_{jG}\right]^{T}\left[{}_{jG}T_{jGV}\right]$$

Gear to A/C Body

$$B^{T}_{LG} = \begin{bmatrix} \cos(P_{MG}) & \sin(P_{MG})\sin(R_{LG}) & \sin(P_{MG})\cos(R_{LG}) \\ 0 & \cos(R_{LG}) & -\sin(R_{LG}) \\ -\sin(P_{MG}) & \cos(P_{MG})\sin(R_{LG}) & \cos(P_{MG})\cos(R_{LG}) \end{bmatrix}$$

$$B^{T}_{NG} = \begin{bmatrix} \cos(P_{NG}) & 0 & \sin(P_{NG}) \\ 0 & 1 & 0 \\ -\sin(P_{NG}) & 0 & \cos(P_{NG}) \end{bmatrix}$$

$$B^{T}_{RG} = \begin{bmatrix} \cos(P_{MG}) & \sin(P_{MG})\sin(R_{RG}) & \sin(P_{MG})\cos(R_{LG}) \\ 0 & \cos(R_{LG}) & -\sin(R_{RG}) \\ -\sin(P_{MG}) & \cos(P_{MG})\sin(R_{RG}) & \cos(P_{MG})\cos(R_{LG}) \end{bmatrix}$$

Gear Velocity to Horizontal

$$H^{T}_{jGV} = \begin{bmatrix} \cos\Psi_{jw} & -\sin\Psi_{jw} & 0 \\ \sin\Psi_{jw} & \cos\Psi_{jw} & 0 \\ 0 & 0 & 0 \end{bmatrix} \qquad j = L, R, N$$

Gear to Gear Velocity

$${}_{jGV}T_{jG} = \left[{}_{jG}T_{jGV}\right]^{-1}$$

GEAR/RUNWAY GEOMETRY

Difference Between Runway Heading and Fuselage Heading

$$\Delta\Psi = \Psi - \Psi_{RWY}$$

Position of cg From End of Runway

$$P_{cg} = N_{RWY} = X_{NORTH}$$

Distance Across Runway From Centerline to cg

$$\Delta CR_{cg} = E_{RWY} = Y_{EAST}$$

Distance Across Runway From cg to Wheels

$$\Delta CR_{LG} = R_{L(1)} \sin\Delta\Psi + R_{L(2)} \cos\Delta\Psi$$

$$\Delta CR_{RG} = R_{R(1)} \sin\Delta\Psi + R_{R(2)} \cos\Delta\Psi$$

$$\Delta CR_{NG} = R_{N(1)} \sin\Delta\Psi$$

Distance Across Runway From Centerline to Wheels

$$CR_{LG} = \Delta CR_{cg} + \Delta CR_{LG}$$

$$CR_{RG} = \Delta CR_{cg} + \Delta CR_{RG}$$

$$CR_{NG} = \Delta CR_{cg} + \Delta CR_{NG}$$

Distance Along Runway From cg to Wheels

$$\Delta P_{LG} = R_{L(2)} \sin\Delta\Psi - R_{L(1)} \cos\Delta\Psi$$

$$\Delta P_{RG} = R_{R(2)} \sin\Delta\Psi - R_{R(1)} \cos\Delta\Psi$$

$$\Delta P_{NG} = R_{N(1)} \cos\Delta\Psi$$

Runway Geometry

$$V_{R(TOTAL)} = \sqrt{V_{RW_1}^2 + V_{RW_2}^2 + V_{RW_3}^2}$$

$$V_{L(TOTAL)} = \sqrt{V_{LW_1}^2 + V_{LW_2}^2 + V_{LW_3}^2}$$

$$V_{N(TOTAL)} = \sqrt{V_{NW_1}^2 + V_{NW_2}^2 + V_{NW_3}^2}$$

Skid Angles

$$\Psi_{RW} = \sin^{-1}\left(V_{RW_2} / V_{R(TOTAL)}\right)$$

$$\Psi_{LW} = \sin^{-1}\left(V_{LW_2} / V_{L(TOTAL)}\right)$$

$$\Psi_{NW} = \sin^{-1}\left(V_{NW_2} / V_{N(TOTAL)}\right)$$

$$SK_{ANG(R)} = \left(\Psi_{RW}\right)(57.3)$$

$$SK_{ANG(L)} = \left(\Psi_{LW}\right)(57.3)$$

$$SK_{ANG(N)} = \left(\Psi_{NW}\right)(57.3) - \sigma_N$$

GEAR FORCES AND MOMENTS

$$\bar{F}_{NG} = \left[{}_{NG}T_{NG}\right] \cdot \bar{F}_{NGV}$$

$$\bar{F}_{LG} = \left[{}_{LG}T_{LG}\right] \cdot \bar{F}_{LGV}$$

$$\bar{F}_{RG} = \left[{}_{RG}T_{RG}\right] \cdot \bar{F}_{RGV}$$

Force Vector Acting on Tires in A/C Body Axis

$$\bar{F}_{NA/C} = \left[B^{T}{}_{NG}\right] \cdot \bar{F}_{NG}$$

$$\bar{F}_{LA/C} = \left[B^{T}{}_{LG}\right] \cdot \bar{F}_{LG}$$

$$\bar{F}_{RA/C} = \left[B^{T}{}_{RG}\right] \cdot \bar{F}_{RG}$$

Total Force Acting at CG as a Result of Gear Action

$$\bar{F}_{GEAR} = \bar{F}_{NA/C} + \bar{F}_{LA/C} + \bar{F}_{RA/C}$$

Moments About CG Due to Force at Wheel

$$\bar{M}_{NA/C} = \bar{R}_{N} \times \bar{F}_{NA/C}$$

$$\bar{M}_{LA/C} = \bar{R}_{L} \times \bar{F}_{LA/C}$$

$$\bar{M}_{RA/C} = \bar{R}_{R} \times \bar{F}_{RA/C}$$

Total Moments Acting at CG as a Result of Gear Action

$$\bar{M}_{GEAR} = \bar{M}_{NA/C} + \bar{M}_{LA/C} + \bar{M}_{RA/C}$$

WHEEL FORCES

Altitude of Wheel Hubs

$$h_{RW} = h_{cg} - R_{R(3)} \cos\phi\cos\theta - R_{R(2)} \sin\phi + R_{R(1)} \sin\theta$$

$$h_{LW} = h_{cg} - R_{L(3)} \cos\phi\cos\theta - R_{L(2)} \sin\phi + R_{L(1)} \sin\theta$$

$$h_{NW} = h_{cg} - R_{N(3)} \cos\phi\cos\theta + R_{N(1)} \sin\theta$$

Height of Runway Crown at Center Line

$$h_{R_{CL}} = \tfrac{1}{2}\, RWY_{W}\, RWY_{S}$$

Height of Runway Crown at Wheels

$$h_{RCRN} = h_{R_{CL}} - \left|CR_{RG}\right| RWY_{S}$$

$$h_{LCRN} = h_{R_{CL}} - \left|CR_{LG}\right| RWY_{S}$$

$$h_{NCRN} = h_{R_{CL}} - \left|CR_{NG}\right| RWY_{S}$$

Number of Data Sectors Between Wheel Location and End of Runway

$$P_{LN} = P_{LRWY} \,/\, {}^{1}_{RGH}$$

$$P_{RN} = P_{RRWY} \,/\, {}^{1}_{RGH}$$

$$P_{NN} = P_{NRWY} \,/\, {}^{1}_{RGH}$$

Position of Wheels Along Runway From EOR Point

$$P_{LRWY} = P_{cg} + \Delta P_{LG}$$

$$P_{RRWY} = P_{cg} + \Delta P_{RG}$$

$$P_{NRWY} = P_{cg} + \Delta P_{NG}$$

Location of Wheels in Roughness Sector

$$P_{LRGH} = P_{LRWY} - IP_{LN}\, {}^{1}_{RGH}$$

$$P_{RRGH} = P_{RRWY} - IP_{RN}\, {}^{1}_{RGH}$$

$$P_{NRGH} = P_{NRWY} - IP_{NN}\, {}^{1}_{RGH}$$

Runway Roughness Heights at Gear Locations

$$h_{LBMP} = f\left(P_{LRGH}\right)$$

$$h_{RBMP} = f\left(P_{RRGH}\right)$$

$$h_{NBMP} = f\left(P_{NRGH}\right)$$

Height of Runway at Location of Wheel

$$h_{RRWY} = h_{RCRN} + \left(h_{RBMP}\right)$$

$$h_{LRWY} = h_{LCRN} + \left(h_{LBMP}\right)$$

$$h_{NRWY} = h_{NCRN} + \left(h_{NBMP}\right)$$

Transform of Z Component of δSTRUT From Gear Velocity to Gear Axis System

$$\dot{d}_{RS3} = \left\{ {}^{PGV}T_{RG_{33}} \dot{\delta}_{STRUT(R)} \right\}$$

$$\dot{d}_{LS3} = \left\{ {}^{LGV}T_{LG_{33}} \dot{\delta}_{STRUT(L)} \right\}$$

$$\dot{d}_{NS3} = \left\{ {}^{NGV}T_{NG_{33}} \dot{\delta}_{STRUT(N)} \right\}$$

Tire Deflection Rates

$$\dot{\delta}_{RT} = V_{RTW(3)} + \dot{d}_{RS3}$$

$$\dot{\delta}_{LT} = V_{LTW(3)} + \dot{d}_{LS3}$$

$$\dot{\delta}_{NT} = V_{NTW(3)} + \dot{d}_{NS3}$$

Tire Damping Forces

$$F_{RTD} = \left\{ C_{TM} \dot{\delta}_{RT} \right\}$$

$$F_{LTD} = \left\{ C_{TM} \dot{\delta}_{LT} \right\}$$

$$F_{NTD} = \left\{ C_{TN} \dot{\delta}_{NT} \right\}$$

Normal Force on Tires at Ground

$$F_{RE} = F_{RTS} + F_{RTD}$$

$$F_{LE} = F_{LTS} + F_{LTD}$$

$$F_{NE} = F_{NTS} + F_{NTD}$$

Deflected Radius of Tires

$$R_{RTD} = \left\{ h_{RW} - h_{RRWY} \right\}_{RTIM}$$

$$R_{LTD} = \left\{ h_{LW} - h_{LRWY} \right\}_{RTIM}$$

$$R_{NTD} = \left\{ h_{NW} - h_{NRWY} \right\}_{RTIN}$$

Tire Deflections

$$\delta_{RT} = R_{TIM} - R_{RTD}$$

$$\delta_{LT} = R_{TIM} - R_{LTD}$$

$$\delta_{NT} = R_{TIN} - R_{NTD}$$

Tire Spring Forces

$$F_{RTS} = k_{TM} \delta_{RT}$$

$$F_{LTS} = k_{TM} \delta_{LT}$$

$$F_{NTS} = k_{TN} \delta_{NT}$$

Wheel Velocities Due to A/C Body Rotations

$$\omega = \begin{Bmatrix} p_B \\ q_B \\ r_B \end{Bmatrix}$$

$$\bar{V}_{NR} = \bar{\omega} \times \bar{R}_N$$

$$\bar{V}_{LR} = \bar{\omega} \times \bar{R}_L$$

$$\bar{V}_{RR} = \bar{\omega} \times \bar{R}_R$$

Wheel Velocities in Local Vertical Axis

$$\bar{V}_{NRE} = \left[B^T LV \right] \bar{V}_{NR}$$

$$\bar{V}_{LRE} = \left[B^T LV \right] \bar{V}_{LR}$$

$$\bar{V}_{RRE} = \left[B^T LV \right] \bar{V}_{RR}$$

Total Velocity at Wheel

$$\bar{V}_{NTW} = \bar{V}_G + \bar{V}_{NRE}$$

$$\bar{V}_{LTW} = \bar{V}_G + \bar{V}_{LRE}$$

$$\bar{V}_{RTW} = \bar{V}_G + \bar{V}_{RRE}$$

where

$$\bar{V}_{G(1)} = \dot{X}_{NORTH}$$

$$\bar{V}_{G(2)} = \dot{Y}_{EAST}$$

$$\bar{V}_{G(3)} = -\dot{h}_{DOWN}$$

GEAR FORCES AND MOMENTS

$$\bar{F}_{NG} = \left[{}_{NG}T_{NG}\right] \cdot \bar{F}_{NGV}$$

$$\bar{F}_{LG} = \left[{}_{LG}T_{LG}\right] \cdot \bar{F}_{LGV}$$

$$\bar{F}_{RG} = \left[{}_{RG}T_{RG}\right] \cdot \bar{F}_{RGV}$$

Force Vector Acting on Tires in A/C Body Axis

$$\bar{F}_{NA/C} = \left[B^{T}{}_{NG}\right] \cdot \bar{F}_{NG}$$

$$\bar{F}_{LA/C} = \left[B^{T}{}_{LG}\right] \cdot \bar{F}_{LG}$$

$$\bar{F}_{RA/C} = \left[B^{T}{}_{RG}\right] \cdot \bar{F}_{RG}$$

Total Force Acting at CG as a Result of Gear Action

$$\bar{F}_{GEAR} = \bar{F}_{NA/C} + \bar{F}_{LA/C} + \bar{F}_{RA/C}$$

Moments About CG Due to Force at Wheel

$$\bar{M}_{NA/C} = \bar{R}_{N} \times \bar{F}_{NA/C}$$

$$\bar{M}_{LA/C} = \bar{R}_{L} \times \bar{F}_{LA/C}$$

$$\bar{M}_{RA/C} = \bar{R}_{R} \times \bar{F}_{RA/C}$$

Total Moments Acting at CG as a Result of Gear Action

$$\bar{M}_{GEAR} = \bar{M}_{NA/C} + \bar{M}_{LA/C} + \bar{M}_{RA/C}$$

WHEEL FORCES

Altitude of Wheel Hubs

$$h_{RW} = h_{cg} - R_{R(3)} \cos\phi\cos\theta - R_{R(2)} \sin\phi + R_{R(1)} \sin\theta$$

$$h_{LW} = h_{cg} - R_{L(3)} \cos\phi\cos\theta - R_{L(2)} \sin\phi + R_{L(1)} \sin\theta$$

$$h_{NW} = h_{cg} - R_{N(3)} \cos\phi\cos\theta + R_{N(1)} \sin\theta$$

Height of Runway Crown at Center Line

$$h_{R_{CL}} = \tfrac{1}{2} \, RWY_{W} \, RWY_{S}$$

Height of Runway Crown at Wheels

$$h_{RCRN} = h_{R_{CL}} - \left|CR_{RG}\right| RWY_{S}$$

$$h_{LCRN} = h_{R_{CL}} - \left|CR_{LG}\right| RWY_{S}$$

$$h_{NCRN} = h_{R_{CL}} - \left|CR_{NG}\right| RWY_{S}$$

Number of Data Sectors Between Wheel Location and End of Runway

$$P_{LN} = P_{LRWY} \,/\, l_{RGH}$$

$$P_{RN} = P_{RRWY} \,/\, l_{RGH}$$

$$P_{NN} = P_{NRWY} \,/\, l_{RGH}$$

Position of Wheels Along Runway From EOR Point

$$P_{LRWY} = P_{cg} + \Delta P_{LG}$$

$$P_{RRWY} = P_{cg} + \Delta P_{RG}$$

$$P_{NRWY} = P_{cg} + \Delta P_{NG}$$

Location of Wheels in Roughness Sector

$$P_{LRGH} = P_{LRWY} - IP_{LN} \, l_{RGH}$$

$$P_{RRGH} = P_{RRWY} - IP_{RN} \, l_{RGH}$$

$$P_{NRGH} = P_{NRWY} - IP_{NN} \, l_{RGH}$$

Runway Roughness Heights at Gear Locations

$$h_{LBMP} = f\left(P_{LRGH}\right)$$

$$h_{RBMP} = f\left(P_{RRGH}\right)$$

$$h_{NBMP} = f\left(P_{NRGH}\right)$$

Height of Runway at Location of Wheel

$$h_{RRWY} = h_{RCRN} + \left\{h_{RBMP}\right\}$$

$$h_{LRWY} = h_{LCRN} + \left\{h_{LBMP}\right\}$$

$$h_{NRWY} = h_{NCRN} + \left\{h_{NBMP}\right\}$$

STRUTS

Strut Forces

$$F_{GW(N)} = -F_{NG(3)}$$

$$F_{GW(L)} = -F_{LG(3)}$$

$$F_{GW(R)} = -F_{RG(3)}$$

Damping Coefficients

$$CV_N = f\left[\delta_{STRUT(N)}\right]$$

$$CV_L = f\left[\delta_{STRUT(L)}\right]$$

$$CV_R = f\left[\delta_{STRUT(R)}\right]$$

Strut Equation of Motion

$$\ddot{\delta}_{STRUT(N)} = \left[\left(F_{GW(1)} - F_{DAMP(N)} - F_{SPRING(N)}\right) / m_{U(N)}\right]$$

$$\ddot{\delta}_{STRUT(L)} = \left[\left(F_{GW(2)} - F_{DAMP(L)} - F_{SPRING(L)}\right) / m_{U(L)}\right]$$

$$\ddot{\delta}_{STRUT(R)} = \left[\left(F_{GW(3)} - F_{DAMP(R)} - F_{SPRING(R)}\right) \quad m_{U(R)}\right]$$

$$F_{DAMP(J)} = \dot{\delta}_{STRUT(J)}\left[C_{DAMP(J)} + CV_J\left|\dot{\delta}_{STRUT(J)}\right|\right]$$

Damping Force

$$F_{DAMP(N)} = \dot{\delta}_{STRUT(N)}\left[C_{DAMP(N)} + CV_N\left|\dot{\delta}_{STRUT(N)}\right|\right]$$

$$F_{DAMP(L)} = \dot{\delta}_{STRUT(L)}\left[C_{DAMP(L)} + CV_L\left|\dot{\delta}_{STRUT(L)}\right|\right]$$

$$F_{DAMP(R)} = \dot{\delta}_{STRUT(R)}\left[C_{DAMP(R)} + CV_R\left|\dot{\delta}_{STRUT(R)}\right|\right]$$

Spring Force

$$\Psi_{GN} = f\left(\delta_{STRUT(N)}\right)$$

$$\Psi_{GL} = f\left(\delta_{STRUT(L)}\right)$$

$$\Psi_{GR} = f\left(\delta_{STRUT(R)}\right)$$

$$F_{SPRING(N)} = \Psi_{GN} \cdot ORF_{AREA(N)}$$

$$F_{SPRING(L)} = \Psi_{GL} \cdot ORF_{AREA(L)}$$

$$F_{SPRING(R)} = \Psi_{GR} \cdot ORF_{AREA(R)}$$

Anti-Skid

$$FB_{ON} = \mu_{DR} F_{RE} / CV_{RCT}$$

$$= \mu_{DL} F_{LE} / CV_{LCT}$$

$$FB_{CMD} = A_{BRK} BKPED_R$$

$$= A_{BRK} BKPED_L$$

$FB_{CMD} = 0.$ for brakes off

RUNWAY CONDITION PROFILES

Side Force Coefficients

$$\mu_{SL} = f\left(SK_{ANG(L)}, V_{LH}\right)$$

$$\mu_{SR} = f\left(SK_{ANG(R)}, V_{RH}\right)$$

$$\mu_{SN} = f\left(SK_{ANG(N)}, V_{NH}\right)$$

Braking Coefficients

$$\mu_{DL} = f\left(SK_{ANG(L)}, V_{LH}\right)$$

$$\mu_{DR} = f\left(SK_{ANG(R)}, V_{RH}\right)$$

$$\mu_{DN} = f\left(SK_{ANG(N)}, V_{NH}\right)$$

$$CY_{RCP} = \max\left(2. - .0164\, V_{R(TOTAL)}, .25\right)$$

$$CY_{LCP} = \max\left(2. - .0164\, V_{L(TOTAL)}, .25\right)$$

$$CY_{RCT} = 1. - .00965 V_{R(TOTAL)} \quad \text{wet, flooded or icy}$$

$$= 1. - .00351\ V_{R(TOTAL)} \quad \text{dry}$$

$$CY_{LCT} = 1. - .00965\ V_{L(TOTAL)} \quad \text{wet, flooded or icy}$$

$$= 1. - .00351\ V_{R(TOTAL)} \quad \text{dry}$$

Braking Forces Due to Friction Acting on Wheels When Brakes are on

$$F_{LB} = \mu_{LD}\, F_{LE}$$

$$F_{RB} = \mu_{RD}\, F_{RE}$$

$$F_{NB} = 0.$$

Velocity Components in Horizontal Plane to A/C Body

$$\bar{V}_{NW} = \left[H^T_{LV}\right] \bar{V}_{NTW}$$

$$\bar{V}_{LW} = \left[H^T_{LV}\right] \bar{V}_{LTW}$$

$$\bar{V}_{RW} = \left[H^T_{LV}\right] \bar{V}_{RTW}$$

Force Vectors at Each Wheel

$$\bar{F}_{jGV} = \begin{Bmatrix} F_{jGV(1)} \\ F_{jGV(2)} \\ F_{jGV(3)} \end{Bmatrix} = \begin{matrix} -F_{jB}\ SSK_j\ \mu_{Sj} \\ -F_{jE}\ SSK_j\ \mu_{S_j} \\ -F_{jE}\ SSK_j\ \mu_{Sj} \end{matrix}$$

Wheel Velocities

$$V_{RH} = \left\{\sqrt{V_{RTW_1}^2 + V_{RTW_2}^2}\right\}$$

$$V_{LH} = \left\{\sqrt{V_{LTW_1}^2 + V_{LTW_2}^2}\right\}$$

$$V_{NH} = \left\{\sqrt{V_{NTW_1}^2 + V_{NTW_2}^2}\right\}$$

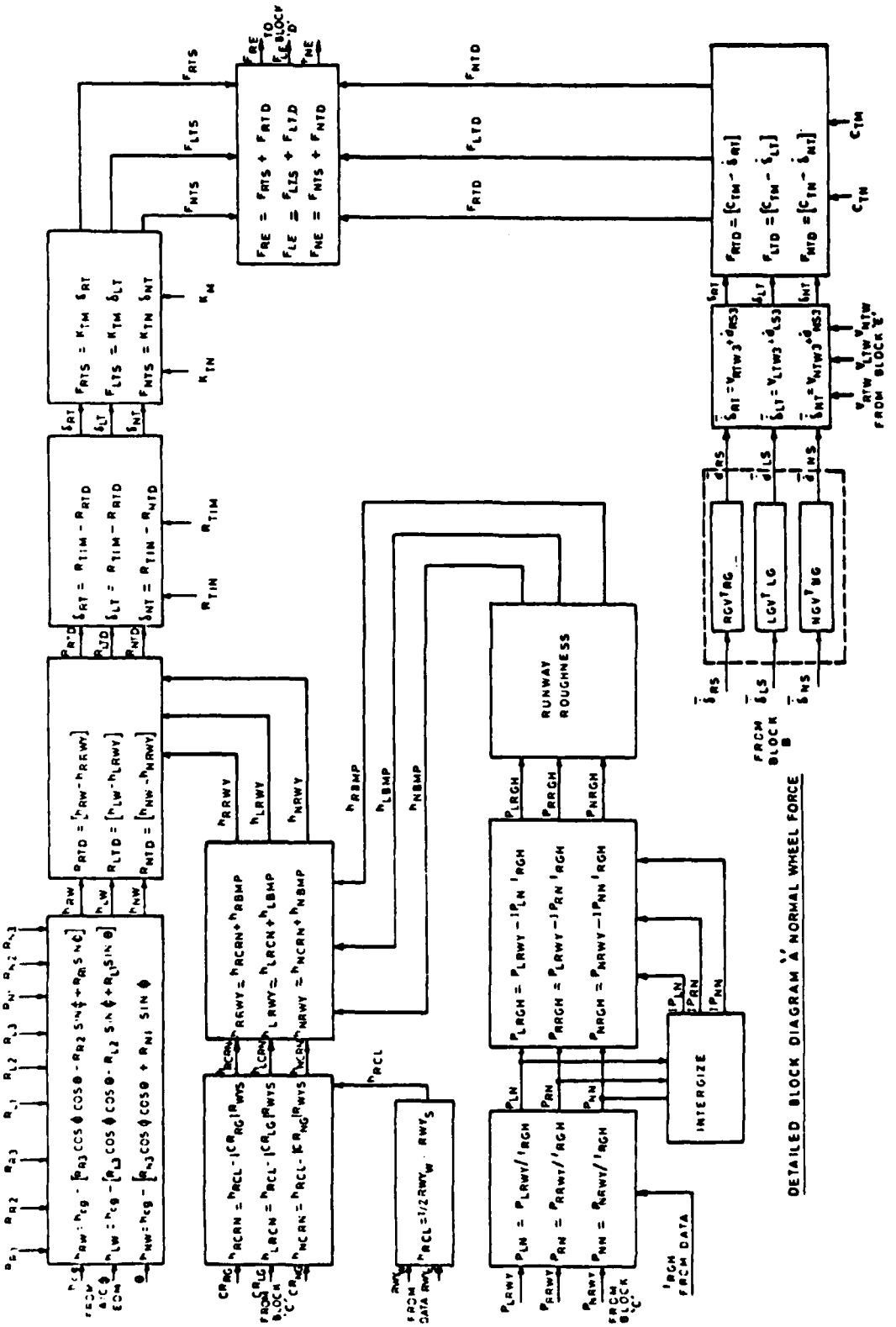

DETAILED BLOCK DIAGRAM 'A' NORMAL WHEEL FORCE

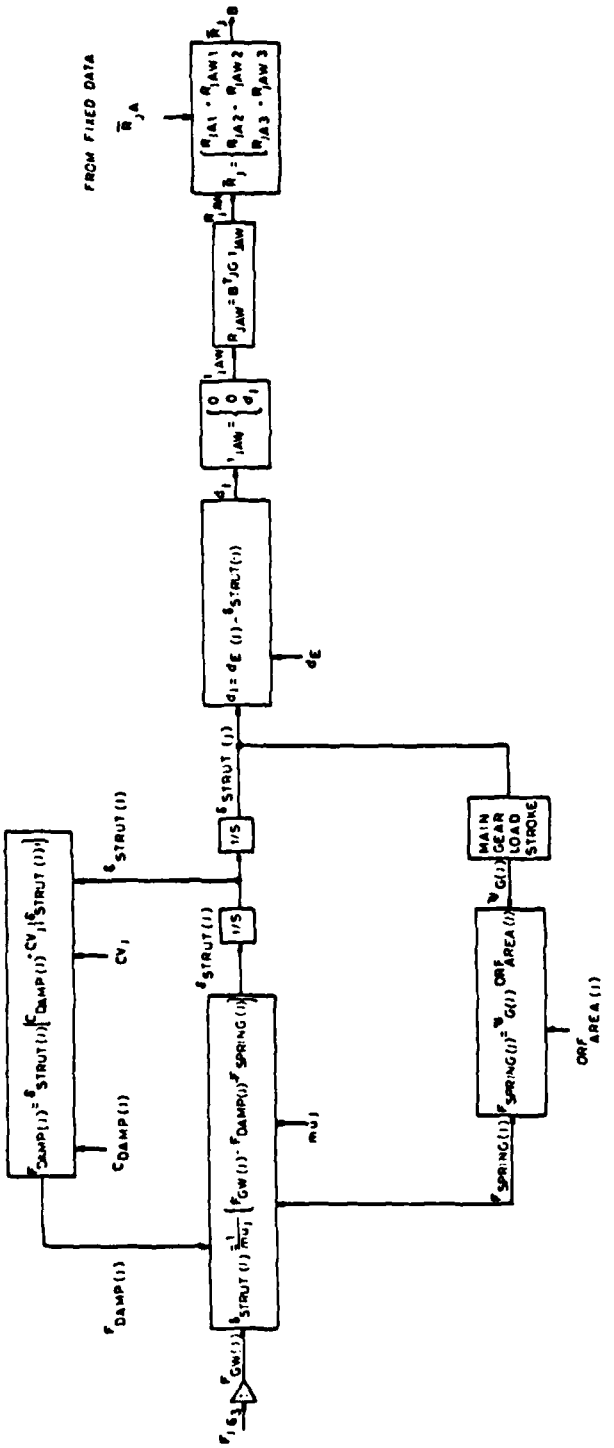

DETAILED BLOCK DIAGRAM 'B' - STRUT DYNAMICS

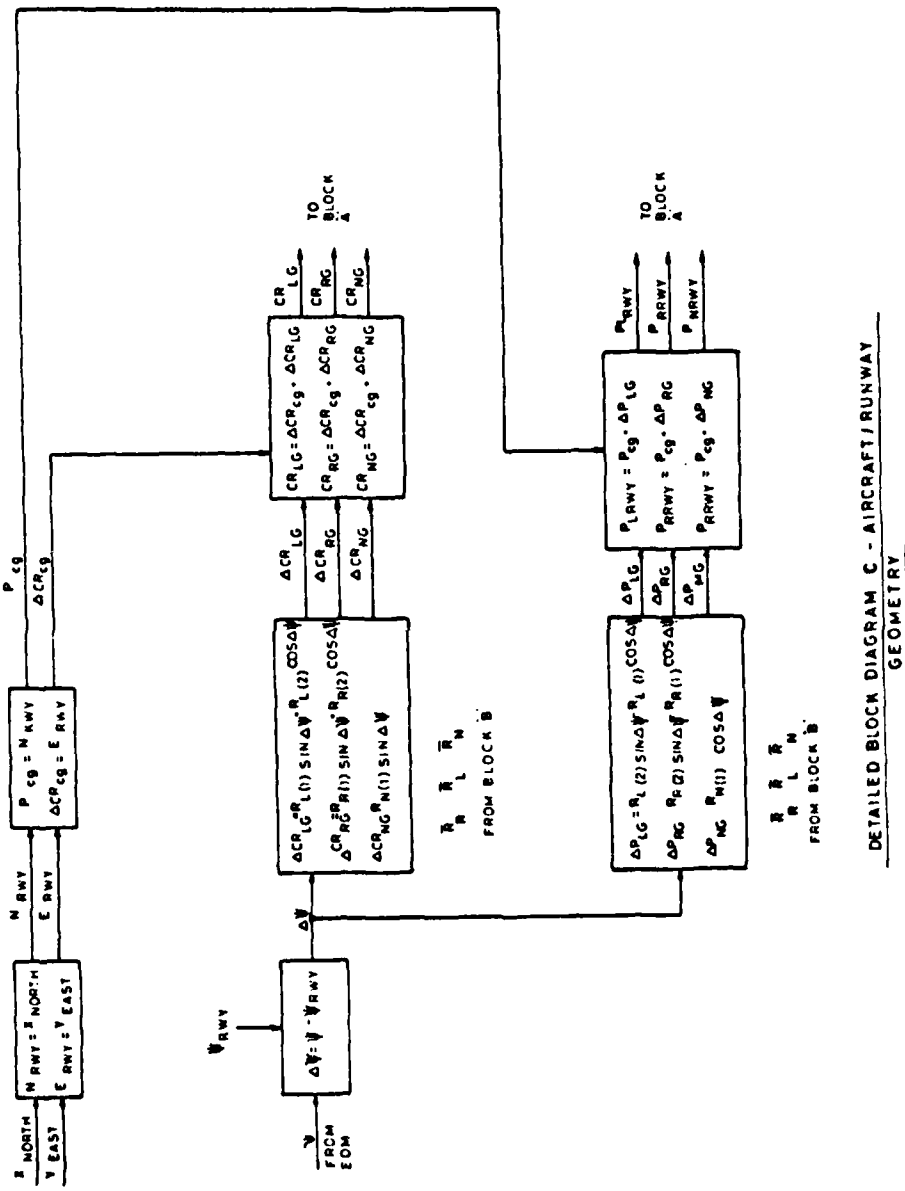

DETAILED BLOCK DIAGRAM C - AIRCRAFT/RUNWAY GEOMETRY

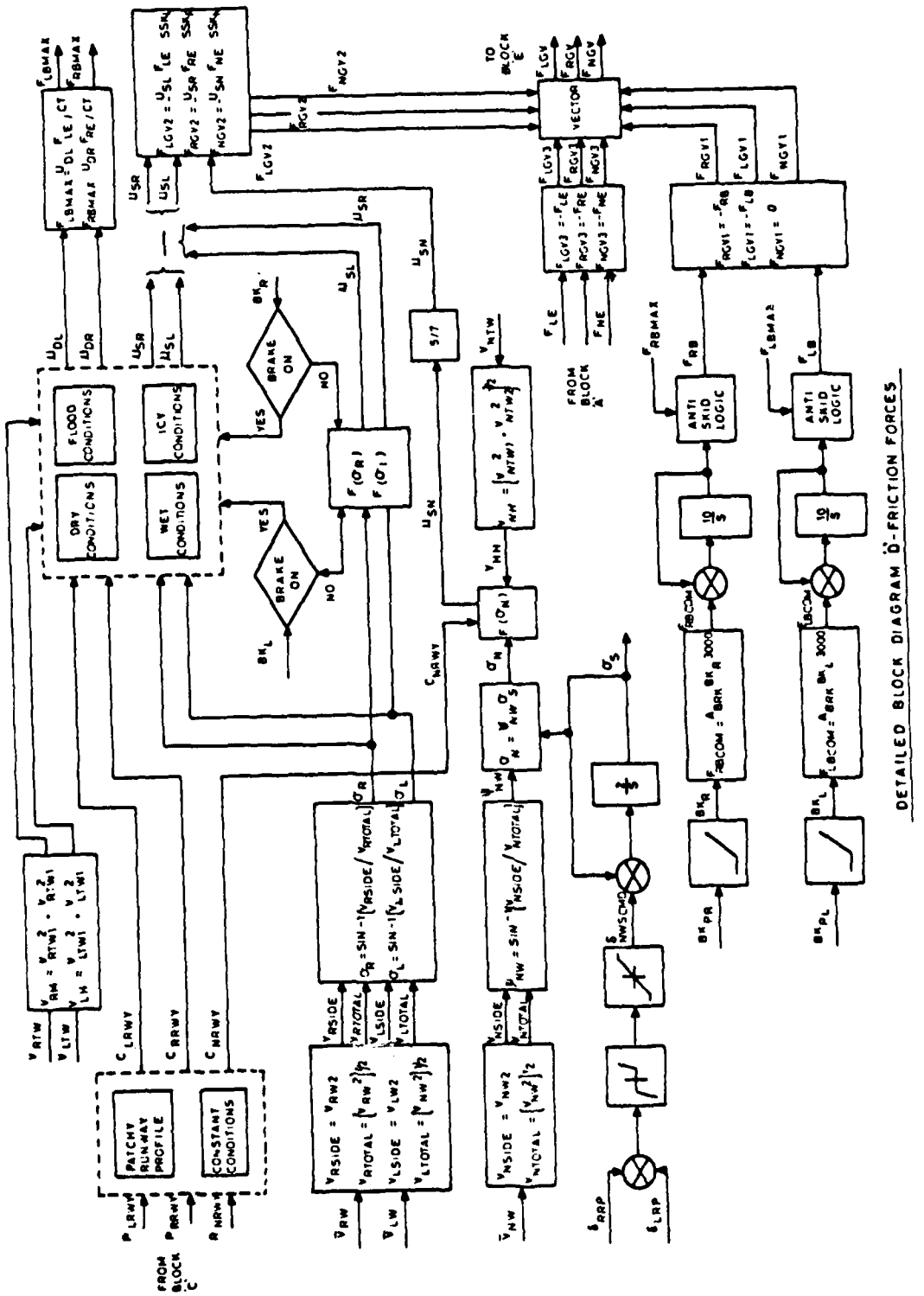

DETAILED BLOCK DIAGRAM Ö-FRICTION FORCES

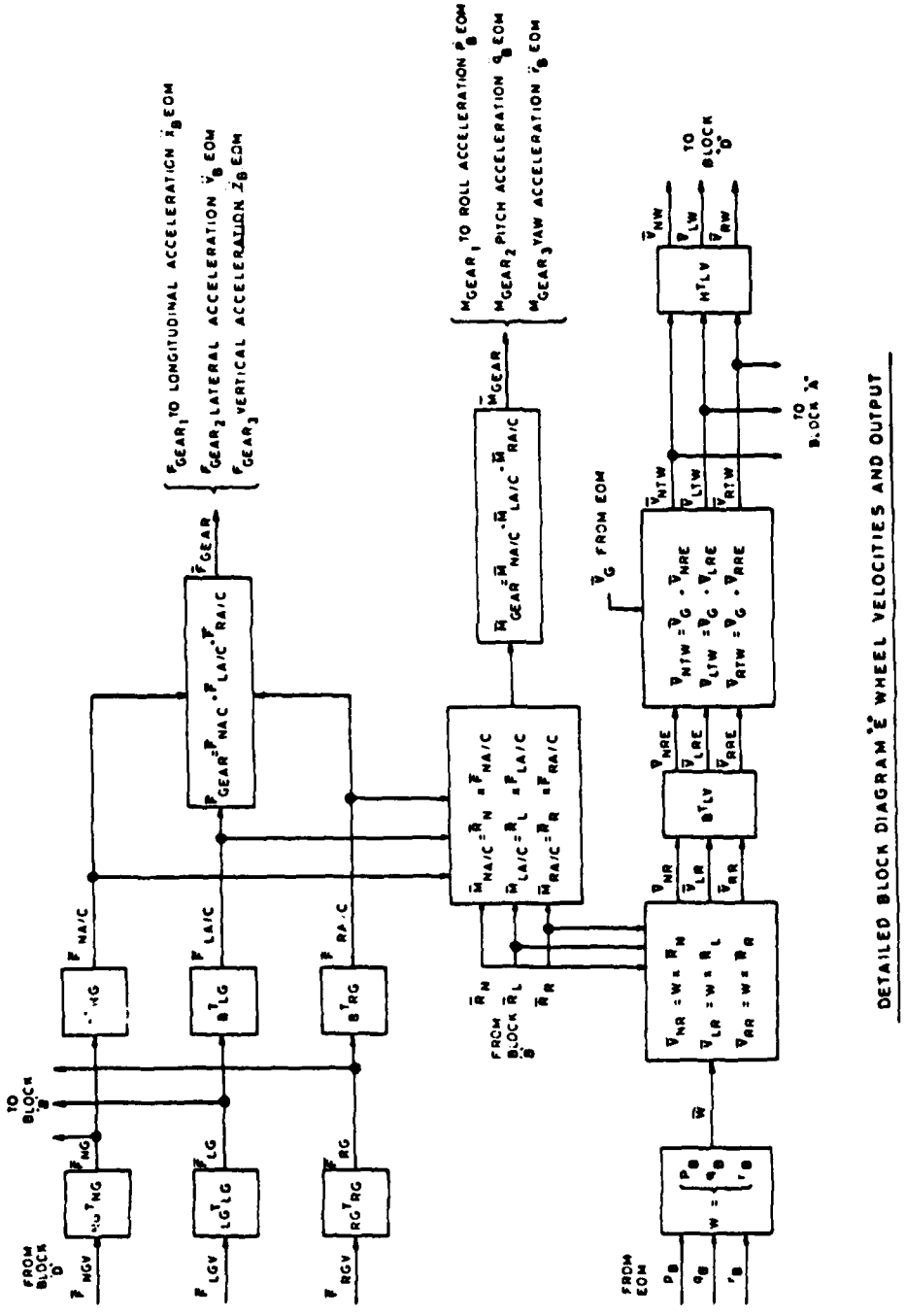

DETAILED BLOCK DIAGRAM 'E' WHEEL VELOCITIES AND OUTPUT

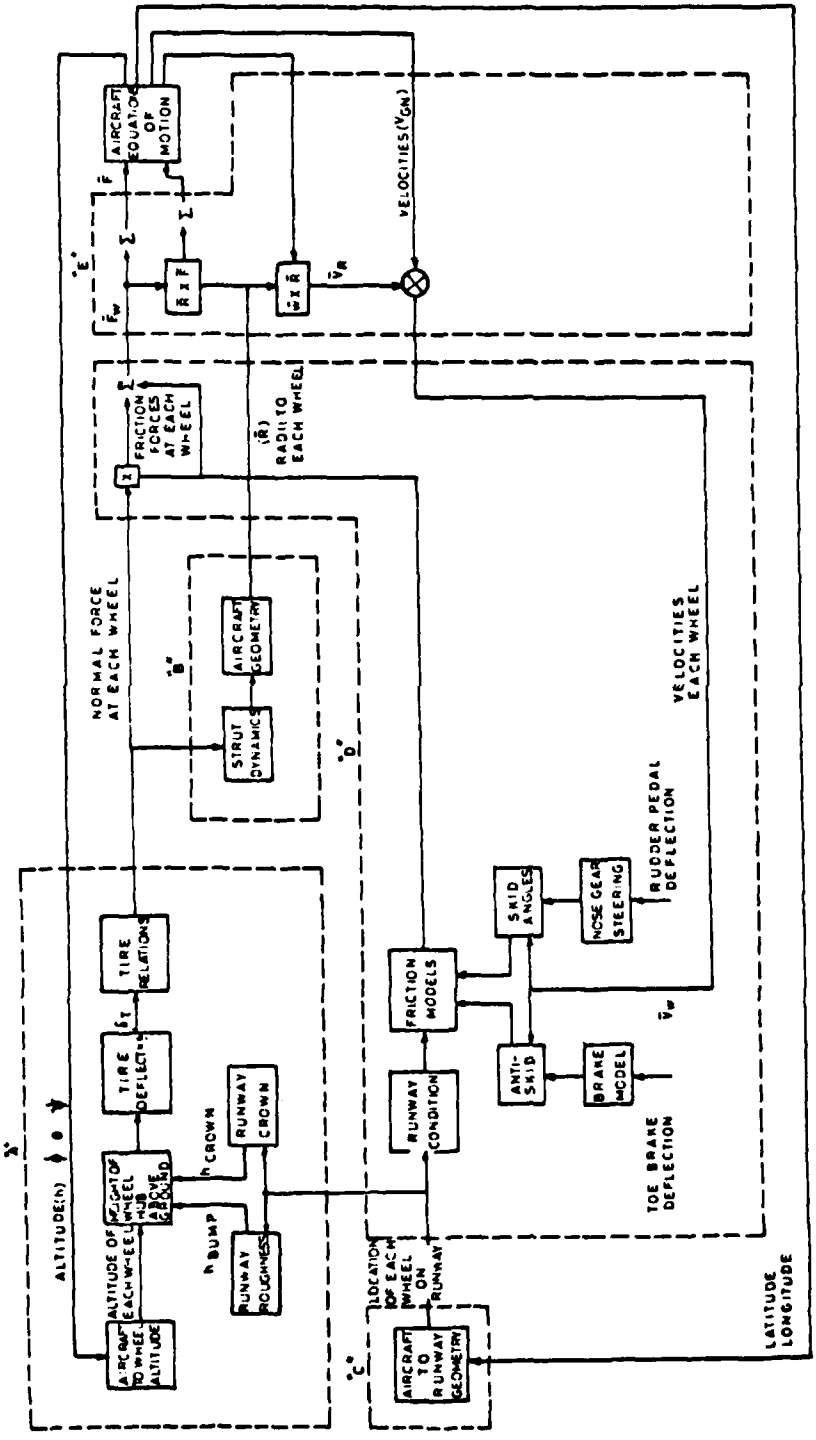

LANDING GEAR MATH MODEL SYSTEM DIAGRAM

REPORT DOCUMENTATION PAGE

1. Recipient's Reference	2. Originator's Reference	3. Further Reference	4. Security Classification of Document
	AGARD-AG-285	ISBN 92-835-1490-4	UNCLASSIFIED

5. Originator Advisory Group for Aerospace Research and Development
North Atlantic Treaty Organization
7 rue Ancelle, 92200 Neuilly sur Seine, France

6. Title
SIMULATION OF AIRCRAFT BEHAVIOUR ON AND CLOSE TO THE GROUND

7. Presented at

8. Author(s)/Editor(s)
A.G.Barnes and T.J.Yager

9. Date
January 1985

10. Author's/Editor's Address Chief Simulation Engineer, British Aerospace Plc, Warton Aerodrome, Preston, Lancs PR4 1AX, UK
Aerospace Technologist, Impact Dynamics Office — MS 497, NASA — Langley Research Center, Hampton VA 23665, USA

11. Pages
64

12. Distribution Statement This document is distributed in accordance with AGARD policies and regulations, which are outlined on the Outside Back Covers of all AGARD publications.

13. Keywords/Descriptors

Aircraft
Flight characteristics
Flight simulation
Mathematical models
Flight simulators
Pilot training

14. Abstract

This AGARDograph provides a guide to the current state of the technology of simulating fixed-wing aircraft handling qualities and performance on or close to the ground, and indicates some of the pitfalls which may prevent an adequate implementation. The scope of possible applications in both aircraft design work and pilot training is indicated and the requirements for mathematical model definitions and implementations are discussed. The current requirements for visual and motion systems, cockpit cueing, and software modelling are also reviewed, and illustrated with specific examples in areas of aircraft research and development studies and pilot training uses. The report conclusions identify needs for further improvements and additional data aquisition.

This AGARDograph has been sponsored by the Flight Mechanics Panel of AGARD.

AGARD AGARDograph 285 Advisory Group for Aerospace Research and Development, NATO SIMULATION OF AIRCRAFT BEHAVIOUR ON AND CLOSE TO THE GROUND by A.G.Barnes and T.J.Yager Published January 1985 64 pages This AGARDograph provides a guide to the current state of the technology of simulating fixed-wing aircraft handling qualities and performance on or close to the ground, and indicates some of the pitfalls which may prevent an adequate implementation. The scope of possible applications in both aircraft design work and pilot training is indicated and the requirements for mathematical model P.T.O	AGARD-AG-285 Aircraft Flight characteristics Flight simulation Mathematical models Flight simulators Pilot training	AGARD AGARDograph 285 Advisory Group for Aerospace Research and Development, NATO SIMULATION OF AIRCRAFT BEHAVIOUR ON AND CLOSE TO THE GROUND by A.G.Barnes and T.J.Yager Published January 1985 64 pages This AGARDograph provides a guide to the current state of the technology of simulating fixed-wing aircraft handling qualities and performance on or close to the ground, and indicates some of the pitfalls which may prevent an adequate implementation. The scope of possible applications in both aircraft design work and pilot training is indicated and the requirements for mathematical model P.T.O	AGARD-AG-285 Aircraft Flight characteristics Flight simulation Mathematical models Flight simulators Pilot training
AGARD AGARDograph 285 Advisory Group for Aerospace Research and Development, NATO SIMULATION OF AIRCRAFT BEHAVIOUR ON AND CLOSE TO THE GROUND by A.G.Barnes and T.J.Yager Published January 1985 64 pages This AGARDograph provides a guide to the current state of the technology of simulating fixed-wing aircraft handling qualities and performance on or close to the ground, and indicates some of the pitfalls which may prevent an adequate implementation. The scope of possible applications in both aircraft design work and pilot training is indicated and the requirements for mathematical model P.T.O	AGARD-AG-285 Aircraft Flight characteristics Flight simulation Mathematical models Flight simulators Pilot training	AGARD AGARDograph 285 Advisory Group for Aerospace Research and Development, NATO SIMULATION OF AIRCRAFT BEHAVIOUR ON AND CLOSE TO THE GROUND by A.G.Barnes and T.J.Yager Published January 1985 64 pages This AGARDograph provides a guide to the current state of the technology of simulating fixed-wing aircraft handling qualities and performance on or close to the ground, and indicates some of the pitfalls which may prevent an adequate implementation. The scope of possible applications in both aircraft design work and pilot training is indicated and the requirements for mathematical model P.T.O	AGARD-AG-285 Aircraft Flight characteristics Flight simulation Mathematical models Flight simulators Pilot training

definitions and implementations are discussed. The current requirements for visual and motion systems, cockpit cueing, and software modelling are also reviewed, and illustrated with specific examples in areas of aircraft research and development studies and pilot training uses. The report conclusions identify needs for further improvements and additional data aquisition.

This AGARDograph has been sponsored by the Flight Mechanics Panel of AGARD.

ISBN 92-835-1490-4

definitions and implementations are discussed. The current requirements for visual and motion systems, cockpit cueing, and software modelling are also reviewed, and illustrated with specific examples in areas of aircraft research and development studies and pilot training uses. The report conclusions identify needs for further improvements and additional data aquisition.

This AGARDograph has been sponsored by the Flight Mechanics Panel of AGARD.

ISBN 92-835-1490-4

definitions and implementations are discussed. The current requirements for visual and motion systems, cockpit cueing, and software modelling are also reviewed, and illustrated with specific examples in areas of aircraft research and development studies and pilot training uses. The report conclusions identify needs for further improvements and additional data aquisition.

This AGARDograph has been sponsored by the Flight Mechanics Panel of AGARD.

ISBN 92-835-1490-4

definitions and implementations are discussed. The current requirements for visual and motion systems, cockpit cueing, and software modelling are also reviewed, and illustrated with specific examples in areas of aircraft research and development studies and pilot training uses. The report conclusions identify needs for further improvements and additional data aquisition.

This AGARDograph has been sponsored by the Flight Mechanics Panel of AGARD.

ISBN 92-835-1490-4

END

FILMED

5-85

DTIC